Finanziato dall'Unione europea NextGenerationEU | Ministero dell'Università e della Ricerca | Italiadomani PIANO NAZIONALE DI RIPRESA E RESILIENZA

multi-Risk sciEnce for resilienT commUnities undeR a changiNgclimate

Codice progetto MUR: **PE00000005** – CUP LEAD PARTNER: J33C22002840002

Deliverable title: Review of relevant data sources and methods for urban multi-risk data fusion and integration

Deliverable ID: 5.2.3

Due date: 31 May 2024

Submission date: 30 May 2024

AUTHORS

Erika Brattich, Federico Porcù, Giorgia Proietti Pelliccia, Tiziano Maestri (UNIBO)

CONTRIBUTORS:

Eva Vanna Lorenza Negri, Francesca Borghi, Francesco De Cataldo, Francesco Violante (UNIBO); Roberto Castelluccio, Antonio Salzano, Rossella Marmo, Enrico Pasquale Zitiello, Maria Carla Fraiese, Ferdinando di Martino, Valeria d'Ambrosio, Vittorio Miraglia, Barbara Cardone, Gabriella Tocchi, Maria Polese (UNINA); Massimiliano Pittore (EURAC)

1. Technical references

Project Acronym	RETURN
Project Title	multi-Risk sciEnce for resilienT commUnities undeR a changiNg climate
Project Coordinator	Domenico Calcaterra UNIVERSITA DEGLI STUDI DI NAPOLI FEDERICO II domcalca@unina.it
Project Duration	December 2022 – November 2025 (36 months)

Deliverable No.	DV5.2.3
Dissemination level*	PU
Work Package	WP2 - Multi-risk oriented modelling of urban systems
Task	T2.3 - Models and methods for urban multi-risk data management
Lead beneficiary	UNIBO
Contributing beneficiary/ies	UNINA, EURAC

PU = Public

PP = Restricted to other programme participants (including the Commission Services)

RE = Restricted to a group specified by the consortium (including the Commission Services)

CO = Confidential, only for members of the consortium (including the Commission Services)

Document history

Version	Date	Lead contributor	Description
0.1	12/05/2024	Erika Brattich, Tiziano Maestri, Federico Porcù, Giorgia Proietti Pelliccia (UNIBO)	First draft
0.2	15/05/2024	Maria Polese (UNINA), Massimiliano Pittore (EURAC), Tiziano Maestri (UNIBO)	Critical review and proofreading
0.3	20/05/2024	All authors	Edits for approval
1.0	29/05/2024	Erika Brattich, Tiziano Maestri, Giorgia Proietti Pelliccia, Andrea Faggi (UNIBO)	Final version

2. ABSTRACT

After presenting the Risk-Oriented Taxonomy and Ontology of Urban Subsystems and Functional Models (DV 5.2.1), and the multi-criteria metrics and methodology for integrated exposure assessment (DV 5.2.2), the purpose of this Deliverable is to identify the relevant indicators and variables needed for risk assessment in the urban and metropolitan settlements, and relevant example algorithms available for risk assessment. Given the wide range of risks present in the urban areas, and the inherent complexities in tackling multi-risks also related with cascade and compound events, an approach based on event risk storylines and related impact chains is presented. As such, the aim of this Deliverable is to present the approach developed for a subset of relevant risk storylines among those presented and described in DV 5.2.1. To this aim, after recalling the main concepts of the previous Deliverables such as the risk definition in terms of hazard, exposure and vulnerability, and the usage of event storylines, a subset of storylines is described, and the main components are described in terms of indicators and variables needed to proceed with risk assessment. After that, some algorithms for risk quantification are outlined, with an aim of identifying characteristics and constraints for the data sources to be used for the risk assessment. In this way, the Deliverable demonstrates the capabilities and the advantages of the approach taken, mainly lying in its modularity and high flexibility thanks to the choice of lying on the event storylines and impact chains. In spite of being not fully exhaustive, as the approach is fully described only for selected branches of a few impact chains, the Deliverable successfully paves the way for the further development within the project, and in particular for the identification of data sources and development of smart data models (DV 5.2.4) and the integration of data from heterogenous sources in WP5, and the development of risk models in WP3. Similarly, as far as the evaluation of risk and the development of risk models are concerned, rather than being exhaustive in the algorithms presented, the Deliverable presents some recommendations and key characteristics on data uncertainty and constraints, thus guiding the next steps in the choice of data sources and development of risk models.

List of Figures

List of Tables

3. Table of contents

4. Introduction

Environmental risk assessment is an approach that stems from ecology and evaluates the likelihood that adverse effects may occur, or are occurring, as a result of exposure of organisms or communities to one or more chemical compounds (e.g., EMA, 2018). The objectives of such assessment are to:

i) Identify potential hazardous areas so that adequate safety measures can be adopted to reduce the likelihood of accidental events;

ii) Identify the stakeholders and evaluate their risk along with proposing adequate control techniques;

iii) Manage the emergency situation or a disastrous event.

Although originally this concept excludes natural calamities and focuses on chemicals and pollutants, it can be quite easily extended to natural and climate hazards, and urban multi-risk evaluation to estimate the probability of an event causing an undesirable effect. Recently, the European Environment Agency and the Directorate-General for Climate Action of the European Commission (DG CLIMA) have launched the European Climate Risk Assessment (EUCRA)[1], aiming at providing a comprehensive assessment of current and future climate change impacts and risks related to the environment, economy and wider society in Europe. Previously, the C40 Cities (C40 Cities, 2018) prepared a concise guide to help cities to conduct a climate change risk assessment (CCRA) in line with requirements of the Global Covenant of Mayors for Climate & Energy (GCoM). The climate risk assessment should include the following components:

- The city's demographic, socio-economic and environmental context, to understand potential impacts and priorities for the city.
- Past climatic events.
- Climate change trends and future scenarios, and research into the likelihood, consequence, frequency and impacts of each hazard type on people and sectors.
- A map of climate risks and vulnerabilities, identifying how and where climate hazards will affect the city, sectors and assets.
- Identification of priority risks, based on exposure, sensitivity, interdependencies and vulnerability.

This simple guide, and the required specified components, clearly highlight that, although risk is a term in everyday use, it is difficult to define it in practice due to the complex interdependencies of its components (Jones and Boer, 2004). Risk is indeed the combination of the likelihood (the probability of occurrence) and the consequences of an adverse event (here, environmental and climate hazard). As such, the major elements of risk are respectively: hazard, probability and vulnerability or hazard, exposure and vulnerability. In both cases, there are two main approaches to assess climate risk, i.e. a natural hazards-based approach and a vulnerability-based approach, depending on the starting emphasis (Jones and Boer, 2004). As noted and detailed in previous RETURN Deliverables (e.g., 5.2.1, 5.2.2), RETURN has adopted a vulnerability-based approach which emphasizes the socio-economic aspect of environmental-related risk.

We recall here briefly the main components of the risk, namely the hazard, vulnerability and exposure definitions.

A **hazard** is an event with a potential to cause harm, such as tropical cyclones, droughts, floods, or conditions leading to an outbreak of disease-causing organisms (plant, animal or human). The UNDRR (United Nations Office for Disaster Risk Reduction) defines hazard as a process, phenomenon or human activity that may cause loss of life, injury or other health impacts, property

damage, social and economic disruption or environmental degradation. Within RETURN we refer to to the hazards´ taxonomy proposed by UNDRR-ISC in 2021 (UNDRR-ISC, 2021).

Exposure According to IPCC (IPCC, 2022), the presence of people; livelihoods; species or ecosystems; environmental functions, services, and resources; infrastructure; or economic, social, or cultural assets in places and settings that could be adversely affected [by one or more hazards]. Exposure can be described in terms of the quantity (number, spatial distribution) and quality (structural and non-structural features) of the exposed assets and systems.

Vulnerability According to IPCC (IPCC, 2022), vulnerability is the propensity or predisposition [of the exposed systems] to be adversely affected. Vulnerability encompasses a variety of concepts and elements, including sensitivity or susceptibility to harm and lack of capacity to cope and adapt. It can relate to flaw or weaknesses in the system under study, and denotes the likelihood that assets will be damaged/destroyed/affected when exposed to a hazard.

Impacts. The consequences of realized risks on natural and human systems, where risks result from the interactions of hazards (including extreme weather/climate events), exposure, and vulnerability. Impacts generally refer to effects on lives, livelihoods, health and well-being, ecosystems and species, economic, social and cultural assets, services (including ecosystem services), and infrastructure. Impacts may be referred to as consequences or outcomes and can be adverse or beneficial (IPCC, 2022).

For each given hazard, it is possible to associate probability with the frequency and magnitude of a given hazard, or with the frequency of exceedance of a given socio-economic criterion (e.g., a threshold). Probability can also range from being qualitative (using descriptions such as “likely” or “highly confident”) to quantified ranges of possible outcomes, to single number probabilities.

In any case and independently on the particular approach adopted, risk assessment and evaluation require not only knowledge of the climate change and environmental hazards across multiple space and timescales (e.g., likelihood of changes to extreme rain over Europe and more specifically over Italy over the next decade), but also knowledge of the exposures (e.g., location of assets and value chains), and of the vulnerabilities (e.g., response of communities to drought or response of supply chain to changes in carbon taxes). To conduct an appropriate assessment also requires the ability to integrate all these heterogeneous sources of information—and their associated and unavoidable uncertainties—to evaluate the effectiveness of possible interventions, helping to communicate risk and prioritise investments (Arribas et al., 2022).

Given the inherent complexities present in risk assessment, and more so within urban environments where exposure and vulnerability elements are intimately related, RETURN has adopted an approach based on risk storylines and impact chains (cfr. Dv 5.2.1). Event-based storylines are defined as physically self-consistent unfoldings of past events, or of plausible future events (e.g., Sillman et al., 2020; Shepherd et al., 2018). This approach is increasingly being adopted in climate risk due to the capability to explore future high-impact events while taking into account aspects of vulnerability and exposure of the considered system with an emphasis on plausibility rather than probability (Sillman et al., 2020). In addition, such an approach can tackle efficiently the uncertainties inherently present in risk assessment, and in particular is capable of:

1) raising awareness on risks by framing risk in an event-oriented rather than in a probabilistic manner, i.e. in a way more directly related to risk perception and response;

2) strengthening decision also addressing compound risks by allowing to work back and forth from a particular vulnerability or decision point, and providing the possibility to combine relevant factors together;

3) providing a physical basis for understanding and estimating uncertainty;

4) exploring the boundaries of plausibility, thus more naturally connected to false alarms, false precision and surprise (Shepherd et al., 2018).

Due to its advantages, this approach has been recently proposed to assess socio-economic responses to remote events (van der Hurk et al., 2023) as well as to analyse and improve flood management (de Brujin et al., 2016) and to bridge the gap between information and decision-making in hydrological risk (Caviedes-Voullième and Shepherd, 2023).

Thus, following the path initiated in RETURN DVs 5.2.1 and 5.2.2, and by adopting the event risk storyline approach, this Deliverable aims at identifying the relevant indicators needed for risk assessment, and the algorithms for quantification of the risk components, for a subset of risk storylines. To this aim, the Deliverable is structured as follows: Section 5 describes the goals and the adopted methodology; Section 6 describes the relevant risk storylines and impact chains selected; Section 7 illustrates the relevant indicators and variables to describe the risk components; Section 8 discusses the algorithms for risk calculation, providing also recommendations in terms of data sources and data constraints; finally, Section 9 draws the main conclusions.

5. Goal and methodology

As stated in the Introduction, the aim of this Deliverable is to identify relevant indicators and algorithms for calculation of risk, with a specific focus on the multiple risks and vulnerability and exposure elements present in the urban environments. This will be taken further in the following DV 5.2.4 (Template and smart data models for data interoperability and pre- and post-event phase collection (including example datasets)), which will describe example data sources, characteristics for the risk calculation. Due to the inherent complexities present in risk assessment, especially in the urban environment, and in order to construct a solid background for the following Tasks in WP3 and WP5, rather than exploring risk in a generic way we have adopted an approach based on risk storylines. In particular, this approach, which stems from climate change research, is increasingly being recognized as providing actionable information, thus very valuable for the aims of RETURN. Indeed, this approach was already successfully adopted in DV 5.2.1 to explore the connection between relevant risks and the specific elements and functions of urban and metropolitan systems. In particular, risk storylines were discussed in a dedicated workshop and are fully described in DV5.2.1 (cfr Appendix A of DV 5.2.1). Each storyline has been designed to focus on a specific urban context and on a specific combination of hazards (possible compound) and cascade impacts.

Storylines are usually based on past events, which provides the opportunity to analyse specific processes and their consequences, highlighting the dependencies and vulnerabilities of the affected systems. However, possible alternative realizations can be equivalently explored, which proves very useful to comprehend and model the impact of relatively rare events with potentially severe consequences (Woo and Johnson, 2023). Event storylines can be alternatively constructed to represent a plausible scenario and have a natural capability of being modularly integrated. As such, RETURN existing storylines have the potential of being integrated in the future, for instance to integrate near misses. Storylines have an essential role of defining the regulative and application framework, the constraints on the risk metrics, aggregation and uncertainty. Thus, the adoption of this approach for this Deliverable will enable to address risk in a very pragmatic way, giving the possibility to extend and develop further the work along the project and beyond. This approach facilitates the adoption of a relatively standard and common methodology for the successive integration of heterogeneous data in RETURN (e.g., WP5, development of data platform and derivatives).

In practice, the methodology of this Deliverable can be described as follows: by selecting a relevant subset of risk storylines among those proposed in DV 5.2.1, indicators for each risk components (hazard, vulnerability and exposure) will be described, along with the variables needed for their calculation; after that, algorithms for the risk calculation will be also described, with a specific focus on the uncertainty and constraints posed by the data. In this way, this Deliverable paves the way to replicate and develop further a concrete methodology for risk calculation for the aims of RETURN.

6. Description of relevant risk storylines and impact chains

In the following, we provide a synthetic description of selected risk storylines and briefly mention the reason of the choice.

The first storyline (storyline 1.2 in DV 5.2.1) describes the risks posed by two independent hazards, namely: heatwave and compound urban and riverine flooding. Key exposed elements are represented by households, and key vulnerabilities are also represented. Below we recall the main urban context and stakeholders involved together with a representation of the impact chain (Figure 1), while for details the reader is referred to DV 5.2.1.

Risk storyline 1:

- Description of the urban context (urban configuration, building typologies, infrastructures, ...): Social housing neighborhood, located on a flood plain.
- Dimension / population (spatial extent in km², resident population, other measures, if known): ~1 km2, 5,000 inhabitants
- Stakeholders: Households, municipality, social housing managers.

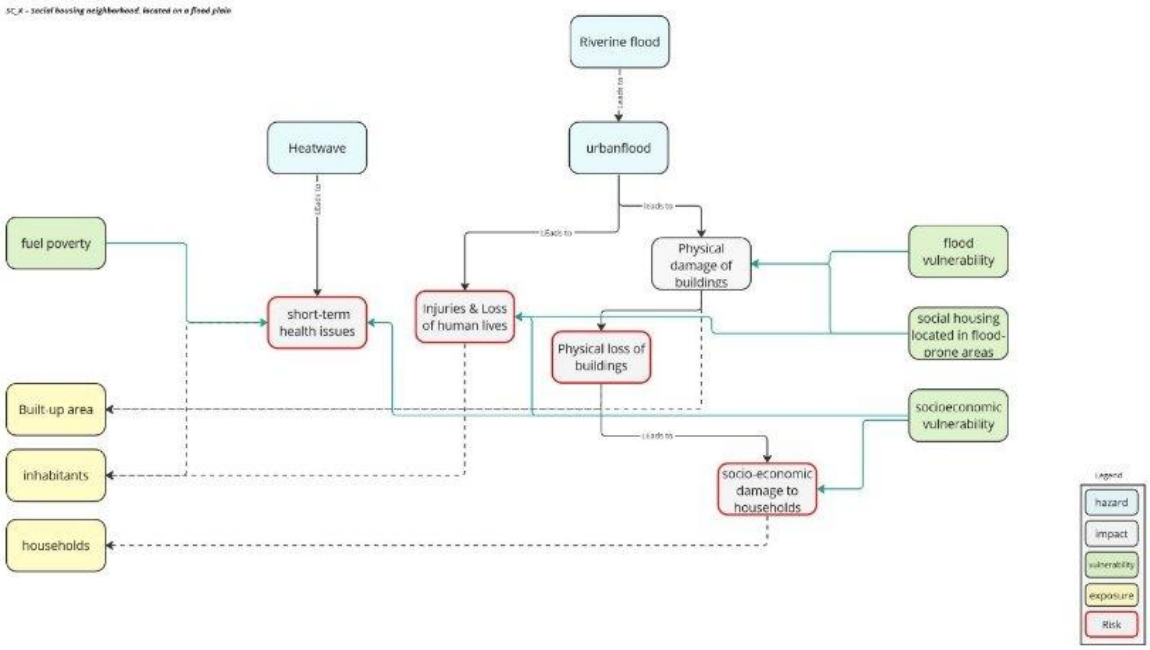

Figure 1. *Impact chain representing the key risk components for the first risk storyline selected in this Deliverable (in the following, storyline 1).*

The second risk storyline herein selected is the one representing the risks posed by seismic events and pluvial floods in a medium-sized town with high population density (Storyline 2 in DV 5.2.1). In this case, key exposed elements include not only the built-up elements, but also the inhabitants. Vulnerability elements are also included in the impact chain below (Figure 2). Again we recall the main urban context and stakeholders involved while for full details of the risk storyline the reader is referred to DV5.2.1.

Risk storyline 2:

- Description of the urban context (urban configuration, building typologies, infrastructures, ...): A medium-sized town with high population density located on a vast low plain, with scattered vegetation and in the absence of rivers. The historic centre is mainly made up of 3 and 4-stories buildings in a compact urban fabric, surrounded by a residential fabric of more recent expansion close to the road infrastructure. Presence of small manufacturing activities in the town and extended farming and agricultural activities in the surrounding lands.
- Dimension / population (spatial extent in km², resident population, other measures, if known): ~50 km2, 50'000 inhabitants
- Stakeholders: Civil Protection department, municipality, inhabitants, small artisans, agricultural industry

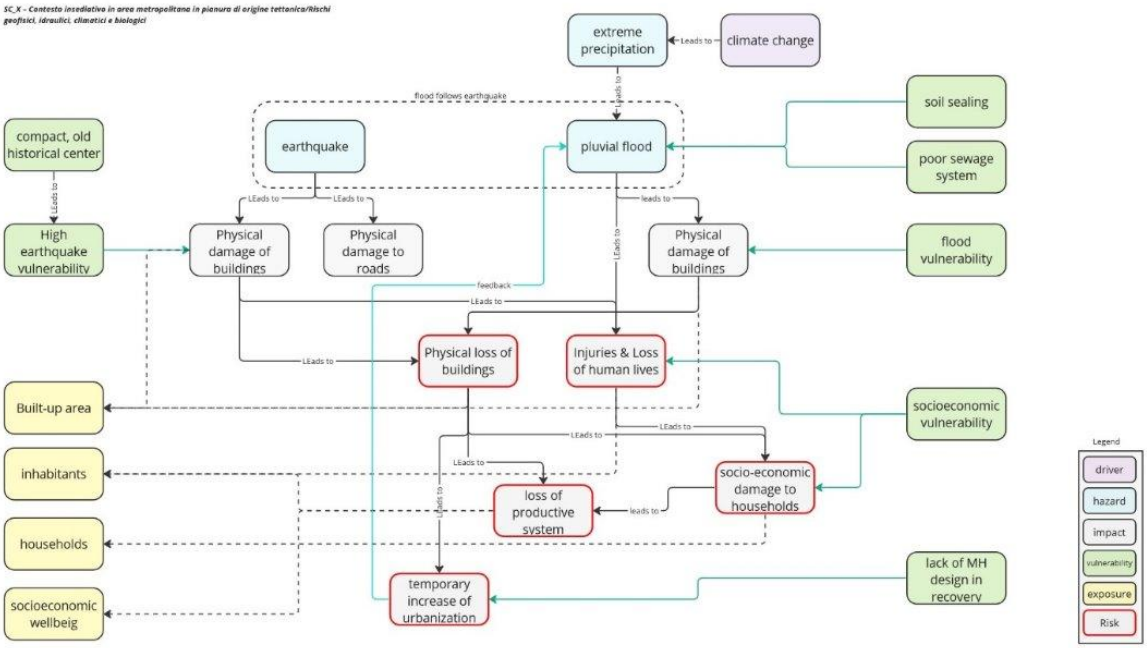

Figure 2. *Impact chain representing the key risk components for the second risk storyline selected in this Deliverable (in the following, storyline 2).*

The two storylines have been selected as examples of different levels of complexity, with the first one relatively simple and the second one more complex. They consider different types of hazards including geophysical and atmospheric hazards. As such, the development of the approach for these two storylines can showcase the capability and advantages of the approach adopted, while maintaining the potential of being extended for other storylines or further integration of these ones.

7. Description of relevant indicators for risk storylines

In the following, we describe the relevant indicators for each risk storyline and in particular for each risk component. For each risk component (colored box in the risk storyline), we start with a broad, but specific, definition, then we list and describe the main indicators.

7.1 Risk storyline 1

In this subsection, we describe relevant indicators for individual risk components in the risk storyline 1.

- **Hazards**
  - *Heatwave*

According to the International Meteorological Vocabulary (WMO, 1992), a heatwave is "a marked warming of the air, or the invasion of very warm air, over a large area; it usually lasts from a few days to a few weeks". The IPCC glossary (IPCC, 2022) defines heatwaves as "a period of abnormally hot weather, often defined with reference to a relative temperature threshold, lasting from two days to months". A recent WMO report (WMO, 2023) providing guidelines for defining and identifying temperature and precipitation related extreme events defined generically a heatwave as "a period of marked and unusually hot weather persisting for at least two consecutive days". Such overall definitions remain extremely broad, and similar to other types of extreme meteorological events, heatwaves should be defined in terms of their characteristics such as intensity (magnitude), duration and extent (geographical area interested). Accordingly, many different indicators exist for defining heatwaves, based on local climatological conditions and in particular on one specific climatological variable (e.g., minimum or maximum temperature) or computed using a combination of multiple variables such as temperature, humidity, and wind speed. Metrics can be also based on fixed or mobile thresholds to define the departure from normal conditions and the extremity of the event (WMO, 2023). Considering the multiple risks posed by heatwaves on human health and economic losses, many indices are also constructed to represent specific impacts or sectors (e.g., human health, agriculture, transport, electricity and power). For the purposes of this specific storyline and given the risks considered for the time being, we will focus mostly on metrics related to human health impacts which are explicitly mentioned in the related impact chain. In particular, as for the assessment of heat on human physiology, several indices are utilized and classified in the following categories:

- Temperature depending indices;
- Thermal comfort indices;
- Spell length indices.

Temperature depending indices group all the indices that depend only on temperature variation, thus not providing any information about the physiological stress but very easy to being computed. Thermal comfort indices combine also other atmospheric variables (e.g., wind speed, humidity) which affect the thermal perception of the human body and the consequent physiological stress. Spell length indices describe the duration and persistence of the events.

A large body of literature is already available on the use of thermal comfort indices and of advantages and disadvantages (e.g., Staiger et al., 2019; Basarin et al., 2020; Costa et al., 2024), but in the following we try to capture the main elements of particular relevance within the context of the RETURN project.

1) Heat and Cold Wave Index

The Heat and Cold Wave Index (HCWI) is used to detect and monitor periods of extreme-temperature anomalies (i.e. heat and cold waves) that can have strong impacts on human activities and health. The HCWI indicator is computed for each location (grid-cell), using the methodology developed by Lavaysse et al. (2018), based on the persistence for at least three consecutive days of events with both daily minimum and maximum temperatures (Tmin and Tmax) above the 90th percentile daily threshold (for heat waves) or below the 10th percentile daily threshold (for cold waves). The threshold values of daily minimum and maximum temperature (Tmin and Tmax) that characterize a heat or cold wave are computed from the observed Tmin and Tmax for that calendar day during a 30-year baseline period (1981-2010). For heat waves, the daily threshold values for Tmin and Tmax are defined as the 90th percentile ("Q90") of the 330 respective temperature values in an 11-day window centred on that day, for all years in the baseline period. For cold waves, the daily threshold values for Tmin and Tmax are defined as the 10th percentile ("Q10") of the 330 temperature values in an 11-day window centred on that day, for all years in the baseline period.

Given a fixed location and a i-th calendar day the HCWI may be computed as follows:

Heat waves $T_{max}^{i} - T_{max}^{90} > 0$ $T_{min}^{i} - T_{min}^{90} > 0$	Heatwaves are defined on the persistence of these two conditions for at least three days.
Cold waves $T_{max}^{i} - T_{max}^{10} < 0$ $T_{min}^{i} - T_{min}^{10} < 0$	Cold waves are defined on the persistence of these two conditions for at least three days.

Here T_{max}^{i} and T_{min}^{i} represent the maximum and minimum temperatures measured in the i-th calendar day, T_{max}^{90} and T_{min}^{90} represent the 90th percentile computed for the i-th calendar day based on a 30-year period (1981-2010) in a 11-day window centered in that day, T_{max}^{10} and T_{min}^{10} represent the 10th percentile computed for the i-th calendar day based on a 30-year period (1981-2010) in a 11-day window centered in that day.

2) Excess heat factor

The excess heat factor (EHF) is a health-relevant heatwave (HW) indicator (Oliveira et al., 2022). The rationale supporting the EHF definition is to identify and quantify extreme temperatures as the three-day mean air temperature deviation from the long-term percentile-based climatology, in a given day of the year (DOY), multiplied by the past month acclimatization index (if > 1) (Nairn and Fawcett, 2014). As a result, the EHF is a quadratic function of both the long-term and short-term air temperature anomalies, and its magnitude reflects the human acclimatization to the local climate. Although the EHF does not include humidity in its calculation, it uses daily mean temperature (TM) as the simple average between the daily maximum (TX) and minimum (TN) temperature values, which is implicitly affected by relative humidity changes; hence, according to the authors (Nairn and Fawcett, 2014), the EHF provides local public health stake-holders with a simpler but efficient method to estimate potential human excess heat exposure levels, compared to other bioclimatic indices, such as the Universal Thermal Climate Index (UTCI) (Zare et al., 2018), the Physiological Equivalent Temperature (PET) (Matzarakis et al., 1999) or Apparent Temperature (AT), which require additional weather variables in their calculations (this are usually used in thermal comfort studies).

The EHF is computed using the daily mean temperature (T). If this temperature is not available through measures, it can be calculated as the average between the maximum and the minimum temperatures measured during the 24-hour period starting at 9 AM on i-th day (Nairn and Fawcett, 2014):

$$T = \frac{T_{max} + T_{min}}{2}$$

T_{max} – maximum air temperature (°C)
T_{min} – minimum air temperature (°C)

In this case the Tmax measure precedes temporally the Tmin measure in the 24-hour period (McGregor et al., 2015).

As mentioned above, the EHF is the product of two components, which consider the temperature deviation from climatology and the month acclimatization of people. These two factors are called respectively **Excess Heat Index significance** (EHIsig) and **Excess Heat Index acclimatization** (EHIacc) (Nairn and Fawcett, 2014).

The **EHIsig** for the i-th day is defined as the difference between the average daily mean temperature for a three-day window and the 95th percentile of daily mean temperature in the base period 1971-2000 (T_i^{95}) (Nairn and Fawcett, 2014; Loridan et al., 2016):

$$EHI_{sig} = \frac{T_i + T_{i-1} + T_{i-2}}{3} - T_i^{95}$$

T_i – daily mean temperature of i-th day (°C)
T_i^{95} – 95th percentile of daily mean temperature in the base period 1971-2000 (°C)

Negative EHIsig values indicate absence of significant difference with respect to the climatological average in terms of heatwaves (Nairn and Fawcett, 2014).

The **EHIacc** for the i-th day is defined as the difference between the average daily mean temperature for a three-day window and the average daily mean temperature for the previous 30 days (Nairn and Fawcett, 2014, Loridan et al., 2016):

$$EHI_{acc} = \frac{T_i + T_{i-1} + T_{i-2}}{3} - \frac{\sum_{k=1}^{30} T_{i-k}}{30}$$

Finally, the EHF can be computed as the product of the previous two indices (Nairn and Fawcett, 2014, Loridan et al., 2016):

$$EHF = \max(EHI_{sig}, 0) \times \max(EHI_{acc}, 1)$$

A warm spell (or a heatwave) is identified when there are at least three consecutive days of positive EHF values (Nairn and Fawcett, 2014).

Nairn and Fawcett defined a severity threshold for EHF computing the 85th percentile (EHF_{85}) from the EHF distribution obtained from a climatological period (in their case 1958-2011) for a certain location. They also designate an extreme severity threshold as $EHF_{85}^{extr} = EHF_{85} \times 3$ (Nairn and Fawcett, 2014).

3) Warm spell duration index

The warm spell duration index is defined by WMO as *the count of days in a span on at least six days where the maximum temperature exceeds the 90th percentile of daily maximum temperature calculated*

for a five-day window centered on each calendar day in the base period 1961-1990 (WMO, 2009). The calculation of this index requires the daily maximum temperature for the i-th day and the climatological 30-year period considered.

4) Heat wave duration index

The heat wave duration index is defined as the period longer than 5 consecutive days in which daily maximum temperature exceeds the average maximum temperature by 5 °C (9 °F), the normal period being 1961–1990 (Frich et al. 2002).

5) Heat index

The heat index (HI), also known as the apparent temperature, is what the temperature feels like to the human body when relative humidity is combined with the air temperature. The heat index was developed in 1978 by George Winterling as the "humiture" and was adopted by the USA's National Weather Service a year later. It is derived from work carried out by Robert G. Steadman. (https://www.weather.gov/ama/heatindex) Heat index is effective when the temperature is greater than 26 °C (80 °F) and RH is at least 40%. (McGregor et al., 2015). The HI can be calculated as follows:

$$\begin{aligned} Heat\ Index\ (°F) = & -42.379 + 2.04901523 * T + 10.14333127 * R + \\ & -0.22475541 * T * R - 6.83783 * 10^{-3} * T^2 - 5.481717 * 10^{-2} * R^2 + \\ & +1.22874 * 10^{-3} * T^2 * R + 8.5282 * 10^{-4} * T * R^2 + \\ & -1.99 * 10^{-6} * T^2 * R^2 \end{aligned}$$

T - air temperature (°F)
R - relative humidity (percentage, i.e. RH = 68.5% means R = 68.5)

Alternatively, if T is expressed in °C:

$$\begin{aligned} Heat\ Index\ (°C) = & -8.7844 + 1.61139411 * T + 2.33854884 * R + \\ & -0.14611605 * T * R - 1.23081 * 10^{-2} * T^2 - 1.642483 * 10^{-2} * R^2 + \\ & +2.21173 * 10^{-3} * T^2 * R + 7.2544 * 10^{-4} * T * R^2 + \\ & -3.58 * 10^{-6} * T^2 * R^2 \end{aligned}$$

T - air temperature (°C)
R - relative humidity (percentage, i.e. RH = 68.5% means R = 68.5)

Heat index measures how the human body feels the hot weather: it is a measure of human body comfort due to the different evaporation rates under different temperature and humidity conditions.Higher values of Heat index result in higher stress on human body where it is also shown a table (Table 1; adapted from heatindex_chart_rh.pdf (noaa.gov)) with Heat index computed for different values of temperature and relative humidity).

Table 1. Heat index range, classification and general effect on people in high risk groups.

Classification	Heat Index Range (°F or °C)	General Effect on People in High Risk Groups
Extremely Hot	HI >= 130 °F HI >= 55 °C	Heat/Sunstroke HIGHLY LIKELY with continued exposure
Very Hot	105 °F < HI < 130 °F 40 °C < HI < 55 °C	Sunstroke, heat cramps, or heat exhaustion LIKELY, and heatstroke POSSIBLE with prolonged exposure and/or physical activity
Hot	90 °F < HI < 105 °F 32 °C < HI < 40 °C	Sunstroke, heat cramps, or heat exhaustion POSSIBLE with prolonged exposure and/or physical activity
Very Warm	80 °F < HI < 89 °F 27 °C < HI < 32 °C	Fatigue POSSIBLE with prolonged exposure and/or physical activity

6) Apparent Temperature

Apparent temperature (AT) is defined as the temperature at the reference humidity level, which produces the same amount of discomfort as that experienced under the current ambient temperature and humidity. The reference is set to be the absolute humidity with dewpoint at 14 °C : when the humidity is higher than the reference then AT will be higher than Ta, otherwise AT will be lower than AT. (McGregor et al., 2015) The AT can be computed through an approximation of a mathematical model of human heat balance and can include the effect of temperature, humidity, wind speed and radiation. The effect of full sun produces a maximum increase in AT of about 8 °C under Australian conditions (McGregor et al., 2015).

The AT can be calculated either with (first eq.) or without (second eq.) radiation:

$$AT = T_a + 0.348 * e - 0.70 * w + 0.70 * \frac{Q}{w + 10} - 4.25$$

$$AT = T_a + 0.33 * e - 0.70 * w - 4.00$$

Ta - air temperature (°C)
e - water vapor pressure (hPa)
w – wind speed at an elevation of 10 m (m/s)
Q – net radiation absorbed per unit area of body surface (W/m^2)

The Heat Index itself can be considered a version of Apparent Temperature.

7) Humidex

The Humidex is similar to the Heat Index and based on an empirical formula considering air temperature and vapor tension instead of the relative humidity, this index calculates a perceived temperature taking into account temperature and humidity conditions. (Masterton J.M, Richardson F.A., 1979)

Humidex can be computed as follows:

$$Humidex = T + 0.5555 * (e - 10)$$

T - air temperature (°C)
e – vapor tension (hPa)

Humidex values can be associated to the degree of comfort according to the table below (Table 2; adapted from McGregor et al., 2015). In general, Humidex is considered extremely high when it reaches 40. For Humidex values in the range 30-39 it is recommended to tone down or modify outdoor activities. (McGregor et al., 2015).

Table 2. *Range of the Humidex and associated degree of comfort.*

Humidex Range	Degree of comfort
Humidex > 54	Heatstroke imminent
46 < Humidex < 54	Dangerous, heatstroke possible
40 < Humidex < 45	Great discomfort, avoid exertion
30 < Humidex < 39	Some discomfort
21 < Humidex < 29	Little discomfort
Humidex < 20	No discomfort

8) Thom discomfort index

The Thom discomfort index indicates the level of discomfort due to the high temperature and its combined effect with relative humidity. It is based on dry-bulb and wet-bulb temperatures (Thom 1959; Epstein and Moran 2006).

$$TDI = 0.5 * T_w + 0.5 * T_a$$

Here T_w is wet-bulb temperature and T_a is air temperature (Eq. 4, Epstein and Moran 2006). T_w can be calculated from moisture information according to Stull (2011):

$$T_w = T * \arctan\left[0.151977 * \sqrt{R + 8.313659}\right] + \arctan[T + R] - \arctan[R - 1.676331] +$$

$$+0.00391838 * R^{\frac{3}{2}} * \arctan[0.023101 * R] - 4.686035$$

T - air temperature (°C)
R - relative humidity (percentage, i.e. RH = 68.5% means R = 68.5)

The arctangent function uses argument values as if they are in radiants (Stull, 2011). Table 3 presents ranges for TDI and related comfort degree.

Table 3. Range of the TDI and associated degree of comfort.

TDI Range	Degree of comfort
TDI > 32	Sanitary emergency due to the very strong discomfort which may cause heat strokes
29 < TDI < 31	The whole population feels a heavy discomfort
27 < TDI < 28	Most population feels discomfort and deterioration of psychophysical conditions
24 < TDI < 26	More than half population feels discomfort
21 < TDI < 23	Less than half population feels discomfort
TDI < 20	No discomfort

The thresholds of bioclimatic discomfort used for the Alert system of ARPAE (Zauli Sajani, S. et al. 2016) were identified through a study of mortality conducted in the urban area of Bologna for the period 1983-2003. In particular, discomfort can be classified as:

- Weak discomfort (TDI < 24), under such condition the population feels discomfort but there are no increases in mortality.
- Discomfort (daily average TDI ~ 25), under thede conditions the weaker sections of the population may experience health effects of various kinds (i.e. headaches, dehydration, etc.) which may result in fatalities in some extreme cases. The total mortality due to natural cases and cardiovascular diseases increases on average by about 15% and mortality due to respiratory causes up to 50%.
- Strong discomfort (TDI ≥ 26 or TDI ≥ 25 for three or more days), under these conditions the categories of persons suffering from heat-related illnesses increase. The total mortality, natural causes and cardiovascular ailments, rise by an average of about 30 %. The mortality from respiratory causes rises of about 80 %.

9) Wet-bulb globe temperature

The Wet-Bulb Globe Temperature (WBGT) is a measure of the heat stress in direct sunlight, which takes into account: temperature, humidity, wind speed, sun angle and cloud cover (solar radiation). This differs from the heat index, which takes into consideration temperature and humidity and is calculated for shady areas. It is measured by a simple three-temperature element device, which consists in: a black-globe thermometer measuring a temperature (T_g) considering the integrated effects of radiation and wind, a thermometer measuring the natural wet-bulb temperature (T_{nwb}), and finally a normal thermometer measuring the air temperature (T_a) in a weather screen. (McGregor et al., 2015) These three elements are combined to compute the wet-bulb globe temperature (WBGT):

$$WBGT = 0.7 * T_{nwb} + 0.2 * T_g + 0.1 * T_a$$

T_{nwb} – natural wet-bulb temperature (°C)
T_g – black-globe temperature (°C)
T_a – air temperature (°C)

Alternatively, there is a simplified formula considering air temperature and humidity which provides an approximation of WBGT under moderately sunny and light-wind conditions:

$$WBGT = 0.567 * T_a + 0.393 * e + 3.94$$

T_a – air temperature (°C)
e – water vapor pressure (hPa)

This approximation may overestimate WBGT in cloudy or windy conditions, or when the sun is low or below horizon; on the other hand, it may underestimate WBGT under clear, full-sun and low-humidity conditions. (McGregor et al., 2015). Table 4 presents WBGT ranges and corresponding recommendations for sport activities.

Table 4. *Wet Bulb Globe Temperature index and corresponding recommendations for sport activities (Brocherie and Millet, 2015)*

WGBT	Recommended sporting activity
<18	No recommendations, unlimited/normal activity
18-24	Increase exercise-to-rest ratio; decrease intensity and total duration of activity
24-28	Activity of unfit, unacclimatized, high-risk subjects should be curtailed
28-30	Activity for all except well acclimatized should be stopped
>30	Cancel or stop all practice

10) Relative strain index

The relative strain index (RSI) was developed by Lee and Henschel (Lee, 1965). It is also a measure of discomfort resulting from the combined effect of temperature and humidity. It assumes a person dressed in a light business suit, walking at a moderate pace in a very light air motion. It is applicable to assess heat stress of manual workers under shelter at various metabolic rates. The RSI can be expressed as (Garin A. et al., 2003; Giles B. D. et al., 1990):

$$RSI = \frac{10.7 + 0.74 * (T - 35)}{44 - e}$$

T – air temperature (°C)
e – partial water vapor pressure (mmHg)

This expression takes as reference a set of standard conditions, namely a person wearing a light business suit, walking at 2 mph (1 m/s) with a wind speed set at 1 knot (0.5 m/s). The following table (Table 5; adapted from Giles et al., 1990) displays the RSI values which are considered the limits of various effects of relative strain (numbers = RSI * 10) for average, acclimatized and old people.

Table 5. *Relative strain index limits for the different persons categories.*

(numbers = RSI * 10)	% of Population	Average Person	Acclimatized Person	Old Person
Comfortable	-	< 1	< 2	1
Discomfort	-	2 ÷ 3	3 ÷ 5	2
Distress	-	4 ÷ 5	6 ÷ 10	3
Failure	-	> 5	> 10	> 3
	100	< 3	< 6	< 1
Performance unaffected	50	< 6	< 11	< 3

	0	> 8	> 14	> 3
Tolerance ceases	0	< 6	< 8	< 2
	50	< 11	< 12	< 5
	100	> 14	> 15	> 5

The terms are qualitatively described as follows (Giles et al., 1990):

- Comfort – thermal neutrality, general satisfaction, no anxiety
- Discomfort – sensation of heat and cold, uncomfortable, feeling unease
- Distress – physical strain, lack of concentration and unsteadiness, pain and suffering
- Failure – loss of physiological equilibrium, changes in pulse rate and temperature possibly leading to collapse, hospitalization
- Performance – capability to perform useful work
- Tolerance – level at which physiological and psychological responses become unacceptable

The three models of people are described as follows (Giles B. D. et al., 1990):

- Average Person – healthy Caucasian male, about 25 years of age, accustomed to a median USA culture with no particular acclimatization to heat
- Acclimatized Person – Greek resident (the study of Giles B. D. et al., 1990 was carried out for Greek cities)
- Old Person – Person over 65 years of age

11) Standard effective temperature

Standard effective temperature (SET) (Ji et al., 2022) is a commonly used index in thermal comfort evaluation. It was established based on two-node model which could reflect thermal regulation process of human body. SET has advantages in environment evaluation compared with ET (only considered the air temperature and relative humidity), in which six parameters, air temperature, radiation temperature, relative humidity, air velocity, metabolic rate and clothing insulation, are converted into a SET index. In the paper published in 1986 (Gagge et al., 1986), Gagge et al. presented the new effective temperature (ET*) and the new standard effective temperature (SET*). Due to its complex definition and calculation method, SET has been revised many times since proposed, and it is necessary to analyze and unify the application of SET index thoroughly (Ji et al., 2022).

ASHRAE Standard 55-2017 defines SET as the temperature of an imaginary environment at RH = 50 %, air speed < 0.1 m/s, and [the mean radiant temperature equals the air temperature], in which the total heat loss from the skin of an imaginary occupant with an activity level of 1.0 met and a clothing level of 0.6 clo is the same as that from a person in the actual environment, with actual clothing and activity level.

SET can be calculated with tools such as the thermal sensation prediction tool by Fountain and Huizenga (1997), the Python package "pythermalcomfort" by Tartarini and Schiavon (2020), or the online CBE Thermal Comfort Tool for ASHRAE 55 by Tartarini et al. (2020) available at https://comfort.cbe.berkeley.edu. The following Table presents SET ranges and corresponding thermal perception and physiological stress.

Table 6. *Standard Effective Temperature (SET) index, the corresponding thermal perception and physiological stress. The colour scale goes from cool (blue) to very hot (dark red).*

SET	Thermal perception	Physiological stress
<17	Cool	Moderate hazard

17-30	Comfortable	No danger
30-34	Warm	Caution
34-37	Hot	Extreme caution
>37	Very hot	Danger

12) Perceived temperature

Perceived Temperature (PT) is an equivalent temperature based on a complete heat budget model of the human body. It has proved its suitability for numerous applications across a wide variety of scales from micro to global and is successfully used both in daily forecasts and climatological studies (Staiger et al., 2012). PT (°C) is the air temperature of a reference environment in which the thermal perception assessed by Predicted Mean Vote (PMV) would be the same as in the actual environment. PT enables an adjustment of clothing from wintry, Icl =1.75 clo, to summery, Icl = 0.50 clo, in order to achieve thermal comfort (PMV = 0). If this is not possible, cold stress or heat stress will occur. In the reference environment, Tmrt (mean radiant temperature) equals Ta (air temperature), and wind velocity is reduced to a slight draught. Water vapor pressure is the same as in the actual environment. In case of condensation in the reference environment, the dew point temperature is set to PT.

PT is calculated according to PMV and Icl values in the three intervals (Staiger et al. 2012; Table 7).

***Table** 7. PT calculation based on PMV and Icl in the three intervals.*

Interval	Regression	PT
Cold Stress	PMV < 0 ; Icl = 1.75 clo	PT = 5.805 + 12.6784 * PMV
Comfort	PMV = 0 ; 0.50 < Icl < 1.75 clo	PT = 21.258 - 9.558 * Icl
Heat Load	PMV > 0 ; Icl = 0.50 clo	PT = 16.826 + 6.183 * PMV

PMV = A * L

A = 0.303 * exp[- 0.036 * M] + 0.0275

L = M – W - (C + R + Ecomf + Ediff) - (Cres + Eres)

Icl: clothing insulation (1 clo = 0.155 m^ 2 K W^-1)

M - metabolic heat produced within the body (W/m^2)
W - portion of mechanic work expended from M (W/m^2)
C - convective loss of sensible heat (W/m^2)
R - loss of sensible heat through radiation (W/m^2)
Ecomf - latent heat loss from sweating under thermal comfort conditions (W/m^2)
Ediff - latent heat transfer from skin due to the natural diffusion of water through the skin (W/m^2)
Cres - convective loss of sensible heat through respiration (W/m^2)
Eres - loss of latent heat through respiration (W/m^2)

PMV may be difficult to compute, hence it can be calculated through the Python package "pythermalcomfort" by Tartarini and Schiavon (2020).

The following table (Table 8; adapted from Staiger et al. 2012) shows the thermo-physiological meaning of PT.

Table 8. Thermo-physiological meaning of Perceived Temperature (PT) adapted from Staiger et al. (2012)

PT (°C)	Thermal perception	Thermo-physiological stress
> 38	Very hot	Extreme heat stress
32 ÷ 38	Hot	Great heat stress
26 ÷ 32	Warm	Moderate heat stress
20 ÷ 26	Slightly warm	Slight heat stress
0 ÷ 20	Comfortable	Comfort possible
-13 ÷ 0	Slightly cool	Slight cold stress
-26 ÷ -13	Cool	Moderate cold stress
-39 ÷ -26	Cold	Great cold stress
< -39	Very cold	Extreme cold stress

13) Physiological equivalent temperature

PET is defined as the air temperature at which, in a typical indoor setting (without wind and solar radiation), the heat budget of the human body is balanced with the same core and skin temperature as under the complex outdoor conditions to be assessed (Höppe, 1999).To calculate PET, it is necessary to calculate the thermal conditions of the body with the Munich Energy-balance Model for Individuals (MEMI), which is an equation system that depends on Tcl (mean surface temperature of clothing), Tsk (mean skin temperature) and Tc (core temperature). PET is the air temperature Ta calculated by considering mean radiant temperature equal to air temperature (Tmrt = Ta), air velocity 0.1 m/s, water vapor pressure 12 hPa (approximately RH = 50% for Ta = 20°C).

Predicted mean vote (PMV) and physiological equivalent temperature (PET) for different grades of thermal perception by human beings and physiological stress on human beings for internal heat production: 80 W and heat transfer resistance of the clothing: 0.9 clo are shown in the following table (Table 9, adapted from Matzarakis A, 1999).

Table 9. Predicted mean vote (PMV) and Physiological Equivalent Temperature (PET) for different grades of thermal perception and physiological stress on human beings for internal heat production (adapted from Matzarakis, 1999).

PMV (°C)	PET (°C)	Thermal perception	Grade of physiological stress
< -3.5	> 4	Very cold	Extreme cold stress
-3.5 ÷ -2.5	4 ÷ 8	Cold	Strong cold stress
-2.5 ÷ -1.5	8 ÷ 13	Cool	Moderate cold stress
-1.5 ÷ -0.5	13 ÷ 18	Slightly cool	Slight cold stress
-0.5 ÷ 0.5	18 ÷ 23	Comfortable	No thermal stress
0.5 ÷ 1.5	23 ÷ 29	Slightly warm	Slight heat stress

1.5 ÷ 2.5	29 ÷ 35	Warm	Moderate heat stress
2.5 ÷ 3.5	35 ÷ 41	Hot	Strong heat stress
> 3.5	> 41	Very hot	Extreme heat stress

The Python package "pythermalcomfort" by Tartarini and Schiavon (2020) provides a useful function which allows the calculation of PET.

14) Universal thermal climate index

The Universal Thermal Climate Index (UTCI) is an equivalent temperature (°C), it is a measure of the human physiological response to the thermal environment. The universal thermal climate index (UTCI) describes the synergistic heat exchanges between the thermal environment and the human body, namely its energy budget, physiology and clothing. UTCI takes into consideration the clothing adaptation of the population in response to actual environmental temperature. There are four variables required to calculate the UTCI: 2m air temperature, 2m dew point temperature (or relative humidity), wind speed at 10m above ground level and mean radiant temperature (MRT). Verification metrics has demonstrated that UTCI city point thresholds at the 95th percentile, exceeded for at least 3 consecutive days both at day- and nighttime (15± 2°C and 34.5 ± 1.5°C, respectively), are successful in identifying the number of the days with excess mortality while minimizing misses and false alarm (Di Napoli et al., 2019).

The UTCI can be expressed in mathematical terms in this way (Bröde P. et al., 2012):

UTCI = Ta + Offset(Ta, Tr, va, pa)

Ta – air temperature
Tr – mean radiant temperature
va – wind speed
pa – water vapor pressure (may be replaced with relative humidity)

The Offset function can be calculated through a sixth-order polynomial (Di Napoli at al., 2020). The Python package "pythermalcomfort" by Tartarini and Schiavon (2020) provides a useful function which allows the calculation of UTCI. The following Table presents UTCI values and corresponding physiological stress.

Table 10. *Universal Thermal Climate Index (UTCI) and the corresponding physiological stress. The colour scale goes from extreme cold stress (dark blue) to extreme heat stress (dark red). (Bröde P. et al., 2012)*

UTCI	Physiological stress
<-40	Extreme cold stress
-27/-40	Very strong cold stress
-13/-27	Strong cold stress
0/-13	Moderate cold stress
0/9	Slight cold stress
9/26	No thermal stress
26/32	Moderate heat stress
32/38	Strong heat stress
38/46	Very strong heat stress
>46	Extreme heat stress

15) Heat Stress Index

The Heat Stress Index (HSI) is a quantitative composite measure which integrates into a single number one or more of the thermal, and/or physical, and personal factors affecting heat transfer between the person and the environment. Many heat stress indices have been developed and these can be classified as those based on physical factors of the environment, thermal comfort assessment, "rational" heat balance equations, and physiological strain (Witherspoon and Goldman, 1974). The daily HSI is evaluated through five parameters (Watts and Kalkstein, 2004):

1. The daily maximum and minimum Apparent Temperature (ATmax and ATmin), i.e. the highest and the lowest values of AT recorded over a 24-hour period.
2. The cooling degree days (CDD), i.e. the sum of the number of degrees above an hourly AT of 18.3 °C over a 24-hour period. This value considers the temperature fluctuations such as the temperature drop due to the onset, a thunderstorm or a cold front. High values of CDD are often associated to periods of lower ATmax but without cooling activity (thunderstorms, cold fronts, etc.).
3. The mean cloud cover (CCmean) represents the average hourly cloud cover values between 1000 to 1800 at LST, which is the daytime during which solar radiation can be affected by cloud cover. CCmean scale is 0.0-8.0, assuming discrete values (0.0, 0.5, 1.0, 1.5 and so on).
4. The number of consecutive days of extreme heat (CONS), i.e. the count of consecutive days in which the ATmax value is at least one standard deviation above a 10-day period (or the reference period chosen).

Each variable distribution is fitted with a statistical distribution, in particular ATmax, ATmin and CDD are approximated by a beta function, CONS by a negative binomial distribution and for CCmean is used an empirical fit (Watts and Kalkstein, 2004). Then the daily percentile of each distribution is calculated and it is defined a SUM function that is defined as the sum of daily percentile:

$$SUM = ATmax + ATmin + CDD + CONS + (1 - CCmean)$$

Then the SUM variable is fitted with a beta function. The final step is to calculate the index values for every summer day within each station's 30-yeart dataset based on the percentile of each SUM value (Watts and Kalkstein, 2004). The daily HSI value is the percentile associated with the location and the daily summed value under the SUM curve (McGregor et al., 2015).

16) Heat wave magnitude index

The Heat Wave Magnitude Index (HWMI) is defined as the maximum magnitude of the heat waves in a year, where heat wave is the period ≥ 3 consecutive days with maximum temperature above the daily threshold for the reference period 1981–2010 (Russo et al., 2014).

The process of calculation of HWMI is structured into the following stages (Russo et al., 2014):

1. Define a daily threshold and calculate it for the reference period 1981-2010.
2. For each specific year select all the heat waves lasting 3 consecutive days or more with the daily temperature exceeding the threshold.
3. Decompose each heat wave into subheat waves lasting 3 days, if the heat wave has a length which is not a multiple of 3 days the last days remaining are grouped into a subheat wave with the consecutive calendar days so that this subheat wave includes 3 days as well.
4. For each subheat wave sum the three daily maximum temperatures.
5. Transform the value obtained for each subheat wave into a probability value (from 0 to 1), this value is now defined as the magnitude of the subheat wave.

6. The magnitude of a heat wave is calculated as the sum of the magnitudes of each subheat waves it contains.
7. The HWMI is then the maximum of all heat wave magnitude for a given year.

17) Mora's threshold

The deadliness threshold is a product of a classification model based on heat-related mortality data from around the world and the associated climatic data, it is simple to use since the threshold can be represented using only dry bulb temperature and relative humidity (Mora et al., 2017). With regard to adding more environmental variables to the model, Mora et al. (2017) was only able to marginally increase classification accuracy when other variables (such as mean daily wind speed, and/or mean daily solar radiation) are added. One of the limitations of this metric is the classification model is only trained with mortality and climatic data, in which other factors such as age and socio-economic conditions are not considered.

In addition, there are indexes that may be used as statistical means to assess climatological changes (also in forecasts and projections) and trends rather than to diagnose and identify heat wave events adverse conditions for exposed people. They are reported in the following.

18) Number of Hot Days

The Number of Hot Days (NHD) is important to assess the heat stress and human discomfort and it represents the number of days per year with a mean air temperature at 2 m above the 75th percentile during the summer months (April to September). The number of days is computed over all months of the year, while the percentile is only computed over the summer months (Copernicus Climate Change Service, https://urbansis.eu/hot-days-per-year/). To be consistent with health impact calculations, the threshold that has been chosen to identify a hot day is the 75th percentile of daily mean temperature during summer. The term hot days has been chosen instead of the more commonly used heat-wave days since we focus on events that happen many times every year. The commonly used term heat wave is usually defined as a more extreme event.

The European Environment Agency in ETC-CCA Technical Paper 1/2020 (Climate-related hazard indices for Europe — Eionet Portal (europa.eu)) describes a similar index based on the exceedances of the daily maximum temperature on a fixed suitable threshold (30 °C) for pan-European applications.

19) Number of Tropical Nights

The Number of Tropical Nights is an index based on the days in which the minimum temperature exceeds 20 °C, according to the European Environment Agency in ETC-CCA Technical Paper 1/2020 (Climate-related hazard indices for Europe — Eionet Portal (europa.eu))

20) Heat Wave Index

The Heat Wave Index (HWI) defines a heat wave as a period lasting at least four days with an average temperature that would only be expected to persist over four days once every 10 years, based on the historical record (United States Environmental Protection Agency, https://www.epa.gov/climate-

indicators/climate-change-indicators-heat-waves). The index value for a given year depends on how often the severe heat waves occur and how widespread they are.

The following Table (Table 11) summarizes the heatwave indicators described in this Deliverable, presenting the main variables needed for their calculation and a color code for the level of complexity for the calculation of the index.

Table 11. *Summary table for the heatwave indicators with variables needed for their calculation and main reference. The color code indicates the level of complexity for the calculation of the indicator (green = easy; yellow = intermediate; red = complex; white = other).*

Indicator	Variables	Reference(s)
Heat and Cold wave index	Daily maximum temperature (°C), Daily minimum temperature (°C)	Lavaysse et al., 2018
Excess Heat Factor (EHF)	Daily mean temperature (°C) OR Daily maximum temperature (°C), Daily minimum temperature (°C)	Oliveira et al., 2022 Zare et al., 2018 Loridan et al., 2016 McGregor et al., 2015 Nairn and Fawcett, 2014
Warm Spell Duration Index (WSDI)	Daily maximum temperature (°C)	WMO, 2009
Heat Wave Duration Index	Daily maximum temperature (°C)	Frich et al., 2002
Heat Index	Air temperature (°F or °C), Relative Humidity (%)	McGregor et al., 2015 https://www.weather.gov/ama/heatindex
Apparent Temperature	Air temperature (°C), Water vapor pressure (hPa), Wind speed at 10 m (m/s), Net radiation absorbed (W/m^2)	McGregor et al., 2015
Humidex	Temperature (°C), Vapor tension (hPa)	McGregor et al., 2015 Masterton and Richardson, 1979
Thom Discomfort Temperature	Wet bulb temperature (°C), Air temperature (°C), Relative Humidity (%)	Stull, 2011 Epstein and Moran 2006, Thom, 1976
Wet-Bulb Globe Temperature	Natural wet-bulb temperature (°C), Black-globe temperature (°C), Air temperature (°C), OR Air temperature (°C) Water vapor pressure (hPa)	McGregor et al., 2015
Relative Strain Index (RSI)	Air temperature (°C), Partial water vapor pressure (mmHg)	Garin et al., 2003 Giles et al., 1990 Lee, 1965
Standard Effective Temperature (SET)	Air temperature (°C), Radiation temperature (°C), Relative Humidity (%), Air velocity (m/s), Metabolic rate,	Ji et al. 2022 Tartarini and Schiavon, 2020 Tartarini, 2020 ASHRAE standard, 2017 Fountain and Huizenga, 1997

	Clothing insulation (clo)	Gagge et al., 1986
Perceived Temperature (PT)	Predicted Mean Vote PMV (°C), Clothing insulation (clo)	Tartarini and Schiavon, 2020 Tartarini, 2020 Steiger et al. 2012
Physiological Equivalent Temperature (PET)	Thermal condition of the body given by the Munich Energy-balance Model for Individuals (MEMI)	Tartarini and Schiavon, 2020 Tartarini, 2020 Höppe, 1999 Matzarakis, 1999
Universal Thermal Climate Index (UTCI)	Air temperature at 2 m (°C), Relative Humidity (%) or Dew point temperature (°C), Wind speed at 10 m (m/s) Mean radiant temperature (°C)	Tartarini and Schiavon, 2020 Tartarini, 2020 Di Napoli et al., 2020 Di Napoli et al., 2019 Bröde et al., 2012
Heat Stress Index (HSI)	Maximum apparent temperature (°C), Minimum apparent temperature (°C), Cooling degree days (°C), Mean cloud cover, Number of consecutive days of extreme heat	McGregor et al., 2015 Watts and Kalkstein, 2004
Heat Wave Magnitude Index (HWMI)	Daily Maximum temperature (°C)	Russo et al., 2014
Mora's threshold	-	Mora et al., 2017
Number of Hot Days	Daily Mean Temperature (°C) OR Daily Maximum Temperature (°C)	ETC-CCA Technical Paper 1/2020
Number of Tropical Nights	Daily Minimum Temperature (°C)	ETC-CCA Technical Paper 1/2020
Heat Wave Index	Daily Mean Temperature (°C)	https://www.epa.gov/climate-indicators/climate-change-indicators-heat-waves

- *Compound riverine and urban flood*

A fluvial (or riverine) flood (MH0007 in the UNDRR-ISC Taxonomy) is a rise, usually brief, in the water level of a stream or water body to a peak from which the water level recedes at a slower rate (WMO, 2012).

Fluvial (riverine) flooding primarily results from an extended precipitation event that occurs at, or upstream from, the affected area. It can also occur when traditional flood-control structures, such as levees and dikes, are overtopped.

Flood indicators are generally used to understand floods from management perspective (Wang et al., 2015). The intensity of specific flood events in a river basin is best described by the use of multiple flood indicators. In general flood events are grouped with cluster analysis techniques to detect groups sharing similar characteristics. Indicators mostly refer to different characteristics related to flood intensity: typical examples are **peak discharge** (the maximum discharge of the flood event)**, peak water level** (he water level corresponding to the peak discharge)**, the maximum 24-h volume** (the maximum water quantity of a 24-h period of the flood event)**, the maximum 72-h volume and the**

total flood volume (the total water quantity of the flood event) and their changes over time. Also, flood duration (i.e., the time span from the beginning to the end of a flood event) is another very important factor that has to be taken into account.

Vojtek (2023) developed a fluvial floods risk index (FFRI) composed of a hazard component and a vulnerability component. In particular, the fluvial flood hazard index (FFHI) was computed based on eight physical-geographical indicators and land cover representing the riverine flood potential and also the frequency of flood events in individual municipalities.

As for the FFHI, eight indicators were chosen, namely: lithology, slope angle, curvature, 5-day maximum rainfall, river density, soil texture, land cover, and number of flood events in municipalities. As for lithology, this is due to the fact that different rock types present a varying degree of permeability. The indicator of the number of flood events by municipalities enables to differentiate the fluvial flood hazard among the municipalities in the study area. Hazard indicators were firstly classified in categories, then their importance was ranked (with 1 as the most important class), and finally the share of each class of the six indicators was calculated for the extent of the municipalities. The share of the class was then multiplied with the corresponding weight using the rank sum method. In the next step, the weighted classes of each of the six hazard indicators were summed in order to have one quantitative value for each indicator and then normalized to the scale [0, 1] using the min–max method.

Furthermore, the rest of the hazard indicators (i.e. river density and number of flood events) contain quantitative data, which were not classified into intervals and, therefore, they were directly normalized to the range [0, 1] using the min–max method.

The FFHI was then calculated based on the weighted linear combination technique, where individual indicators were multiplied with their corresponding normalized weights and then aggregated into the respective index.

- **Exposure**

In general, the evaluation of the exposed assets in the urban and metropolitan settlements require description of the population, characteristics of buildings, roads and railroads, and other types of built-up areas.

  - *Built-up area*

The extent, spatial and morphological features characterizing the built-up area possibly exposed to the considered hazards. This might include the number and typologies of single buildings, as well as more spatially aggregated descriptions at a district scale. The recorded structural and non-structural characteristics should be relevant to describe the vulnerability of the structures to the specific hazards. For instance, in the case of heatvawes, insulation properties, type of windows and presence/absence of climatization systems would be required to better estimate the impact on the inhabitants. Especially in the case of floods, it is particularly relevant to divide built-up areas in terms of presence and number of strategic buildings, residential buildings, commercial and industrial buildings, cultural heritage, roads and railroads and environment. As for roads and railroads, the approach developed in the MOVIDA project (https://sites.google.com/view/movida-project/methodology/exposed-assets?authuser=0) and then transposed to the VS1 Water in RETURN stems from the fact that the functional damage linked to the practicability of a road or a railway is often more relevant than the physical damages to the infrastructure. In this case, thus, a damage matrix resulting from the combination of the impact of the flood event in terms of slowdown or interruption of vehicular transit (depending on the hazardous variables; i.e. hydraulic load or water depth) and the uniqueness of the

performance services offered by the infrastructure, depending on the type of flooded section is calculated as a weighted average. This requires the identification of the transport networks in Open Street Map (OSM), further integrated with information from the Regional Geoportal on technical and mechanical characteristics of the network. In this way, transport networks and sections are characterized in terms of importance (e.g., highways, main, secondary, ...) and topographic characteristics (elevation, bridges, viaducts, tunnels, ...).

As for strategic buildings, it is important to distinguish them according to their function for civil protection purposes and for housing vulnerable groups of population, with potential implication in the emergency management. This type of information is generally gathered from national and regional databases, eventually combined with non-institutional sources such as OSM.

In the case of residential buildings, characteristics in terms of footprint area, number of floors, building use, construction material, maintenance level are generally gathered from census data provided by ISTAT. Conversely, in the case of commercial and industrial activities not only the structure of the buildings but also their contents such as machinery, tools and equipment are evaluated.

In terms of environmental areas it is important to classify areas according to the main ecosystem service provided (provisioning, regulation, recreational). Information is gathered from international, national and local open data repositories.

- *Inhabitants*

The number, spatial distribution and characteristics of the people residing in the target area and possibly exposed to the hazards. The specific characteristics could refer to demographic or socio-economic traits or other features relevant for describing the vulnerability of inhabitants to the considered hazards. For instance, to estimate impacts related to heatwaves, but also to some extent for floods, age would be a relevant parameter. Such information can be found in censuses, albeit usually in aggregated form. In this case, uniform population distribution within the census section can be assumed.

- *Households*

A household consists of one or more persons who live in the same dwelling. It may be of a single family or another type of person group. Size, composition, socio-cultural and economic characteristics of households are important to describe social and economic vulnerability. As for inhabitants, this information can be found in censuses, albeit usually in aggregated form.

- **Vulnerability**
  - *Fuel poverty*

It refers to the fuel poverty population density (non-income earners, unemployed and households with more than five members) by census area. In general, this results from three key factors, namely: low household income, poor heating and insulation standards, and high energy prices. In general, fuel poverty measures are classified in: (i) Non-income-based objective/quantitative indicators; (ii) income-based objective/quantitative indicators; (iii) subjective/qualitative indicators; and (iv) subjective/qualitative indicators (Besagni and Borgarello, 2019). To gain a complete of fuel poverty issues, it is necessary to compute all of them. However, from a practical point of view, indicators are

primarily objective/income based and include: (i) The "10% indicator"; (ii) the "minimum income standard (MIS) indicator"; and (iii) the "low income/high cost indicator". According to the **"10% indicator"** (Boardman, 1991), a household is classified as fuel poor if more than 10% of the income is devoted to energy supply. Despite this measure having the great advantage of simplicity, it suffers from different shortcomings: (i) it is highly related to energy prices (which are variable with time); (ii) the 10% threshold is related to the UK economic situation in the 1980s; (iii) the income value is not considered; (iv) socio-demographic and geographic dimensions are not considered; and (v) the dwelling characteristics and type are not taken into account. The **MIS indicator** (Moore, 2012) overcomes some of these limitations, and classifies a household as fuel poor if it does not have enough income to pay for the "basic" energy costs, after covering housing and other needs. Although this measure overcomes some of the limitations, a major disadvantage is still present due to the analytical representation of the relationships between the "Minimum Income Standard" value and the dwelling characteristics and socio-demographic variables. Finally, the **low income/high cost indicator** (Hills, 2012) identifies a fuel poor situation to be when the household income is lower than a "poverty threshold" and the energy-consumption expenditure is higher than a certain threshold. In spite this measure is quite precise, it is affected by relevant limitations: (i) the necessity to define two thresholds; (ii) the negligence of the effects of energy expenditure/consumption reduction (i.e., energy-efficiency measures); (iii) the fact of being based on a theoretical cost (i.e., the requested energy consumption/expenditure to ensure certain internal conditions) rather than on the actual energy consumption/expenditure; and (iv) the potential lack of attention of the most vulnerable people (i.e., the elderly) (Middlemiss, 2017). Alternative measures include for instance: the **after fuel cost poverty indicator** (Heindl, 2015; Hills, 2012; Romero et al., 2015), which defines a household as fuel poor when its income, after energy-consumption and household expenditures, is below a minimum value (defined based on the household variables); the **hidden energy poverty indicator** (Rademaekers et al., 2016), which defines fuel poor households when their energy expenditure is below half of the median expenditure for households with similar characteristics. Recent research (Besagni and Borgarello, 2019) has suggested to use a multiscale approach, by applying different indicators of fuel poverty to a household segmentation, based on a nationally-representative survey, and the adoption of a novel indicator based on the "**minimum thermal comfort**" constraint (Faiella et al., 2017). This constraint compares the minimum energy expenditure to reach a minimum level of comfort conditions with the annual real energy expenditure. While the former represents a theoretical household thermal requirement which can be derived from the application of a lumped parameter model to the whole national building stock, the latter can be based on data available from nationally representative surveys (e.g., "Household Budget Survey" from the Italian National Institute of Statistics (ISTAT, 2017). In this way, this indicator combines the demand and the supply sides.

Thus, the "minimum thermal comfort" constraint indicator couples the demand side and the supply side and potentially appliable to multiple spatial scales from the "household scale" up to the whole "country scale".

- *Flood vulnerability*

The previously cited paper from Vojtek (2023) developed a fluvial flood risk index (FFRI) from a hazard component (previously described) and a vulnerability component. The fluvial flood vulnerability index (FFVI) was calculated using seven indicators representing the economic and social vulnerability of municipalities, including assets and people. In particular, these are: (1) population density of urban areas of municipalities, (2) share of population included in the age category 65+ from the total population of municipality, (3) share of unemployed persons from the total number of economically active population in municipality, (4) share of the Roma ethnicity from the total

population of municipality, (5) the number of buildings within 100 m from a river, (6) length of roads within 100 m from a river, and (7) number of bridges in municipality.

In particular, indicators for economic vulnerability are represented by distance from a river, length of roads within 100 m from a river, number of bridges. Age was considered crucial for social vulnerability to pluvial floods because of the inherent decline in physical strength and mobility and the tendency for elderly people to live alone. In addition, employment level represents a further central characteristic due to the reduced possibility of recovering from a flood event for people with low or no income. The Roma ethnicity was associated with increased vulnerability, mainly due to the construction of colonies close to water streams, poor quality of dwelling and overcrowding.

Similar to the construction of the FFHI, and considering that all vulnerability indicators contain quantitative data, they were normalized to the range [0, 1] using the min–max method. The FFVI was finally calculated as the FFHI based on the weighted linear combination technique, where individual indicators were multiplied with their corresponding normalized weights and then aggregated into the respective index.

Usman Kaoje et al. (2021) also considered flood and building characteristics together with environment characteristics to describe flood vulnerability. In particular, the choice of the indicators and subindicators to develop flood vulnerability indicators was based on a preliminary expert opinion survey form conducted on all the potential indicators obtained from the literature review. The experts assigned a score of relevance (10 point scale) to the indicators and sub-indicators based on their understanding, expertise, and experience on flood vulnerability in the study area. Table 12 presents the preliminary identified indicators for flood vulnerability and the final choice in the paper of Usman Kaoje et al. (2021). Of relevance here it is important to note that they included also flood hazard intensity and related indicators among vulnerability indicators for convenience.

Table 12. *Expert opinion agreement on physical flood vulnerability indicators from Usman Kaoje et al. (2021).*

Description	Indicators	Decision
Characteristics of buildings	Construction type and material	Selected
	Number of floors	Selected
	Presence of basement	Rejected
	Basement windows/opening	Rejected
	Height of opening from the ground	Rejected
	Age of building	Rejected
	Type/Use of building	Rejected
	Building size	Rejected
	Level of Maintenance/condition	Rejected
	Height of the building	Rejected
	Stilts/Elevated buildings	Selected
	Ground floor foundation material	Selected
Flood hazard intensity (I)	Flood water depth	Selected
	Flood duration	Selected
	Flood water Velocity	Selected
	Water sedimentation	Rejected
	Flood return period	Rejected
	Building distance from the coasts	Rejected

Surrounding environment (E)	Building row towards river	Rejected
	Building surrounding fence	Rejected
	Building surrounding vegetation	Rejected
	Distance from main river	Selected
	Terrain elevation	Rejected
	Drainage system	Rejected
	Existence of mitigation measures	Rejected

After selection, a model for the weighting and aggregation of the indicators into the vulnerability index was developed, considering that the physical flood vulnerability of buildings have different levels of relevance in generating flood vulnerability.

- *Socioeconomic vulnerability*

Socioeconomic vulnerability to heatwaves describes the fact that heatwaves particularly endanger low-income households (Osberghaus and Abeling, 2022). To depict this aspect, it is generally needed to obtain statistics of population and/or GDP in the heatwave area (Cai et al., 2021), or data on health status.

In the following we report some of the indicators we plan to use in RETURN.

A widely used metric to reflect socioeconomic vulnerability to extreme heat is the **deprivation index** (Rosano et al., 2020), sometimes used in combination with heat exposure index (Rey et al., 2009) or with other variables reflecting social vulnerability (Krstic et al., 2017; Lopez-Bueno et al., 2021). This index can be computed at the municipality level or at administrative levels below municipality, from the permanent population census. In general, it is constructed from a combination of different indicators of social and economic status, including for instance employment level, age, and education level (e.g., Henderson et al., 2022; Lopez-Bueno et al., 2021). One of the most widely used index for deprivation index is the **Townsend Score** (Townsend, 1987), which is based on four variables, i.e.: unemployed residents as a percentage of all economically active residents; households that do not own a car as a percentage of all households; households that do not own a home as a percentage of all households; and household overcrowding, i.e., more than one person per room. This indicator is used in combination with social isolation proxies (e.g., proportion of single households) and educational level (e.g., proportion of population with no high school diploma) (Buscail et al., 2012). For instance, in the UK (Townsend deprivation index (restore.ac.uk)) the index is constructed from the following four census variables, each of which must be divided by the appropriate count of households or persons to obtain a percentage score. The exact census counts to be used will vary slightly for different censuses.

- Households without a car
- Overcrowded households
- Households not owner-occupied
- Persons unemployed

The unemployment and overcrowding percentages (+1) are then subjected to a log transformation in order to normalise the raw values, which tend to be highly skewed. All four variables are then standardized using a Z-score (subtract the mean value and divide by the standard deviation). These four standardized scores are then summed to obtain a single value which is the Townsend deprivation index. Positive values of the index will indicate areas with high material deprivation, whereas those with negative values will indicate relative affluence. A score of 0 represents an area with overall mean values.

When calculating Townsend scores, it is necessary to know the mean and standard deviation for each variable for the appropriate geographical units across a large reference area - typically the whole country. The score can be standardized over smaller areas, such as a region, but this will not produce nationally comparable values.

Typical indicators for the health status include: the mortality by cause, the hospital admissions and in particular the number of accesses to emergency district, and health atlases published by local health authorities. However, these indicators are often available only at municipality level, and subjected to several privacy and ethical restrictions which potentially hinder their possible use.

- **Risks**
  - *Short-term health issues*

In this case, although heatwaves can result in many risks to several sectors including human health, ecosystems, economic losses due to shortages of the power system and agricultural production, we are mainly concerned with the prediction of the short-term health issues. Relevant indicators to be quantified include the short term increase in mortality/morbidity.

  - *Injuries & loss of human lives*
  - *Physical damage of buildings*
  - *Physical loss of buildings*
  - *Socio-economic damage to households*
  -

7.2 Risk storyline 2

In this subsection, we describe relevant indicators for individual risk components in the risk storyline 2.

- **Hazards**
  - *Earthquake*

An earthquake is "a violent and abrupt shaking of the ground, caused by movement between tectonic plates along a fault line in the earth's crust"[1]. Seismic indicators are generally computed using the temporal sequence of past earthquakes, recorded in earthquake catalog (Asim et al., 2018). In order to generate earthquake predictions, seismic indicators are provided to computationally intelligent algorithms eventually leading to creation of Earthquake Predictor System regarding forthcoming earthquakes. Seismic hazard indicator can be derived from a measure of earthquake-induced ground shaking at the selected scale (e.g., census tract level, district level, municipal level), which is quantified according to a selected hazard map. For instance, the value of peak ground acceleration (PGA) or spectral acceleration at reference elastic periods (Sa(T)) corresponding to an exceedance probability in a given period of time or, equally, to an assigned return period (e.g., 475 years return period or 10% probability of exceedance in 50 years) can be selected as measure of ground shaking. In Italy the official reference for seismic hazard is the **MPS04 model** proposed by Stucchi et al. (2004; 2011). MPS04 hazard maps (provided by INGV[2]) report the seismic hazard (PGA and Sa(T)) corresponding to nine different probabilities of exceedance of the ground motion intensity in 50 years (2%, 5%, 10%, 22%, 30%, 39%, 50%, 63%, 81%), over a grid of more than 16,000 points.

[1] Earthquakes (who.int)
[2] http://esse1.mi.ingv.it/d2.html

- *Extreme precipitation*

The ETTCDI (Expert Team on Climate Change Detection and Indices[3]) has defined several extreme precipitation indices, which are reported in the following Table. Similar to heat waves, indices can describe different hazard characteristics such as duration indices, counter indices, percentile-based indices, absolute indices.

Table 13. *Extreme precipitation climate indices recommended by the ETCDDI.*

Category	Index	Name	Definition	Unit
Duration indices	CWD	Consecutive Wet days	Maximum number of consecutive wet days (i.e. when R ≥ 1 mm)	Days
Counter indices	R10mm	Number of heavy precipitation days	Annual count of days when precipitation ≥ 10 mm	Days
	R20mm	Number of very heavy precipitation days	Annual count of days when precipitation ≥ 20 mm	Days
Percentile-based indices	R95p	Very wet days	Annual total precipitation when daily precipitation > 95th percentile	mm
	R99p	Extremely wet days	Annual total precipitation when daily precipitation > 99th percentile	mm
Absolute indices	Rx1day	Maximum 1-day rainfall total	Annual maximum 1-day precipitation	mm
	Rx5day	Max 5-day precipitation amount	Annual maximum consecutive 5-day precipitation	mm
	PRCPTOT	Annual wet-day precipitation	Annual total precipitation in wet day (rainfall ≥ 1 mm)	mm
Simple index	SDII	Simple daily intensity index	Total rainfall divided by the number of wet days (i.e. average rainfall	mm/day

[3] https://etccdi.pacificclimate.org/list_27_indices.shtml

			of the on days with rainfall ≥ 1 mm)	

Those indices have been widely used to study observed and modeled climate variability across the globe (e.g., Eini et al., 2022; de Medeiros et al., 2022; Myhre et al., 2019) can be calculated through dedicated R or Python libraries (e.g., "CDT: Climate Data Tools." and "RClimDex" in R, "ClimateIndex" in Pyhton).

- *Pluvial flood*

See risk storyline 1.

- **Exposure**
  - *Built-up area*

The characterization of the exposed built-up area can be generic, just including the number of buildings and surface area/living area at census tract level (from ISTAT[4]) or aggregated at larger scale (e.g., municipal level), or also considering the use of specific construction material (i.e., masonry, reinforced concrete, other), number of floors and age of construction.

  - *Inhabitants*

In this case, indicators for the exposed population may be generic including just the number of inhabitants at census tract level (from ISTAT).

  - *Households*
  - *Socioeconomic wellbeing*

  - **Vulnerability**
    - *Compact, old historical center // earthquake vulnerability*

Under this item, we need to describe the physical vulnerability to earthquakes such as: information on structural system, e.g., the construction material of vertical structure and the code design level; building height; horizontal structure types (e.g., flexible or rigid slabs, vaults). Index-based based approaches to evaluate seismic vulnerability of buildings are also available (e.g., the **Risk-UE approach** by Lagomarsino & Giovinazzi, 2006). Other indicators potentially of interest, if data are available, include the following: Infills (fragility, mass); Roof cornice (shape factor, mass); Balcony (shape factor, mass); Roof covering (mass, fragility, joints characteristics); Openings/windows (area, wedge gasket); Household drain system (changes in direction, element span).

    - *Soil sealing*
    - *Poor sewage system*
    - *Flood vulnerability*
    - *Lack of MH design in recovery*

[4] National Institute of Statistics

- *Socioeconomic vulnerability*

As previously illustrated for heatwaves, socioeconomic status may amplify risks to earthquake and flood hazards. In addition to the indicators previously described for risk storyline 1, in the case of earthquakes and pluvial floods, indicators for socioeconomic vulnerability include the **Social vulnerability indicator** (SoVI), derived using the approach proposed by Frigerio et al. (2018). The SoVI is specifically composed of sub-indicators that capture municipality-level information on population age (e.g., rate of elderly older than 65 years), family structure (e.g., family with more than five members), employment (e.g., unemployment rate), socioeconomic status (e.g., commuting rate), ethnicity (i.e., foreign resident), education level and population density, which are obtained from the latest census, and others. In particular, the original formulation of this index (Cutter et al., 2003) considers 42 independent variables subsequently reduced to 11 components applying principal component analysis (PCA). Frigerio et al. (2018) adapted the formulation to the Italian context, starting from the same basic constructs but based on data available in Italy and their relevance to the country's situation. Specifically, the variables were chosen to describe aspects of the Italian population's socioeconomic characteristics that increase or decrease social vulnerability. In particular, the final variables' selection is based on a compromise between data availability for the three census periods considered (the same variables for each year) and their contribution to better explain the social vulnerability of the Italian population. The following Table (Table 14), extracted from Frigerio et al. (2018) represents the variables used in the SoVI index for Italy.

Table 14. *Variables used in the social vulnerability index for Italy (Frigerio et al., 2018)*

Variables	Indicators	Impact on social vulnerability
Family with more than 6 members	Family structure	Increase
High education index	Education	Decrease
Low education index		Increase
Quality of buildings (buildings from 1972)	Socioeconomic status	Decrease
Commuting rate		Increase
Employed female labor force	Employment	Decrease
Employed labor force		
Unemployment rate		Increase
Rate of children < 14 years	Age	Increase
Rate of elderly > 65 years		
Aging index		
Dependency ratio		
Population density	Population growth	Increase
Built-up areas		
Crowding index		
Foreign residents	Race/Ethnicity	Increase

Due to the use of different measurement units in the subindicators, prior to applying the PCA, subindicators need to be normalized. Specifically, the approach foresees the normalization via the djusted Mazziotta–Pareto index (AMPI) method, which enables to appreciate absolute change over time (Mazziotta and Pareto, 2015). Ater that, indicators were input to PCA in order to reduce the dimensionality of the indicators and extract the first principal components by year. A final composite indicator is then extracted as a result of the PCA, providingthe Social Vulnerability Index for each

year. In general the results show that, in agreement with previous research from Frigerio and De Amicis (2016) and Frigerio et al. (2016), vulnerability of the Italian population is best described by age and employment rate.

- **Impact**
  - *Physical damage of buildings*

This specific impact refers to the seismic physical damage to buildings, which can be calculated as the damage attained by structural and non-structural elements (e.g., infills). For characterizing the damage to buildings, a damage scale is usually defined. The **European Macroseismic Scale** (EMS-98) (Grünthal 1998) is often utilized. It defines five damage states Dk (k = 1–5), describing the damage to both structural and non-structural components. For this, a final indicator could consist in the number of buildings reaching a given damage state. To this aim, also the mean damage value can be adopted, which considers the damage distribution for a given intensity level (Lagomarsino & Giovinazzi, 2006).

As an alternative or additional impact indicator, buildings usability determines if people can return home or need to find temporary shelter, and whether buildings can be occupied, either wholly or in part. Building usability is often determined by damage attained by structural and non-structural elements. This aspect is generally described in terms of number of short-term unusable buildings (which required short-term counter-measures to make them safe for use) and number of long-term unusable buildings (they required important structural interventions or even demolition).

A third item refers to the physical damage of building envelope technical elements, which can be considered as a subset of the main impact "physical damage of buildings". In this case, the indicator is the number of performed interventions (e.g., from the fire safety department).

  - *Physical damage to roads*

As previously reported, the functional damage linked to the practicability of a road or railway section is in many cases of greater importance than the physical damages suffered by the infrastructure, thus, a specific methodology needs to be developed for the estimation of the functional damage (i.e., null, low, medium, high impact) expected to the network.

- **Risk**
  - *Physical loss of buildings*

This includes the direct economic losses (€/m^2) due to buildings structural damage, and a relevant subset describing the economic losses due to collapsed building envelope technical elements. In both cases, the indicator to be quantified is the money spent for the interventions. As described previously, specific methods need to be developed according to the different building types and the specific services they provide (residential, commercial and industrial, cultural heritage).

  - *Injuries and loss of human lives*

In this case, this risk includes the injuries and loss of human lives due building structural damages, and its subset injuries and loss of human lives due to collapsed building envelope technical elements (this is a sub-set of the main risk "injuries and loss of human lives". In both cases, the indicator to be quantified is the number of injuries or loss of human lives (e.g., pre-hospital emergency services data sources).

  - *Loss of productive systems*

In the case of commercial and industrial activities, the damages and risks need to consider both the building structure as well as the content. In particular, the economic value of the assets is obtained by multiplying the number of employees within each census block by the unitary net capital (per employee), whose value is derived from data provided by the Italian National Institute of Statistics (ISTAT) at the national level.

- *Socio-economic damage to households*
- *Temporary increase of urbanization*

The following Table summarizes the main individual seismic risk components in the risk storyline 2.

Table 15. *Summary table for the individual seismic risk components in the risk storyline 2. The table shows the indicators with variables needed for their calculation and main reference.*

INDICATOR	VARIABLES	REFERENCES
Seismic hazard	Peak ground acceleration (PGA) or spectral acceleration at reference elastic periods (Sa(T))	Stucchi et al. (2004;2011)
Seismic vulnerability	Material of vertical Structures, lateral load resisting system, type of horizontal structure, roofs.	Di Pasquale et al. (2005); Rosti et al. (2022); Del Gaudio et al., (2019; 2020); Lagomarsino and Giovinazzo, (2006).
Social vulnerability	Population age, socio-economic status, family structure, employment, population growth, ethnicity.	Frigerio et al. (2018)
Exposure – built-up area	Number of buildings and living area; number of inhabitants.	ISTAT (2011)
Exposure - Inhabitants	Number of inhabitants.	ISTAT (2011)
Physical damage	Number/percentages of buildings reaching a given damage state; Mean damage considering the damage distribution for a given intensity level.	Grünthal, (1998); FEMA, (2015); Lagomarsino and Giovinazzi, (2006).
Physical loss of buildings	Losses (€/m2) due to buildings structural damage	Dolce et al. (2021); FEMA (2003).
Injuries and loss of human lives	Injuries and casualties caused by collapsed or severe damaged buildings.	Zuccaro and Cacace (2011), Dolce et al. (2021).

8. Description of relevant algorithms for risk calculation

In this section, we describe relevant algorithms for risk calculation in the two selected risk storylines, with a specific aim to highlight constraints on data and uncertainties deriving from the use of the previously described indicators. Risk assessment and development of quantitative risk maps require the use of data on the indicators previously described. The final output is a quantitative risk assessment expressed in terms of a number (Papathoma-Köhle et al. 2016a, b). In cases data are not available, alternative qualitative risk assessments resulting in a qualitative description (very high, high, medium, low) are possible (Papathoma-Köhle et al. 2016a).

8.1 Risk storyline 1

Several research works have worked on the quantification of the short term health issues arising from extreme heat temperatures. Indeed, also due to the increasing frequency and severity of this type of extreme events, several authors have attempted to construct models for the quantification, and eventually prediction, of their impacts. While the methods generally differ in terms of the indicators adopted, in all cases the final aim is to construct a map of health risk. To this scope, all methods for risk calculation rely on combination (i.e., products or sums) of the risk components, following normalization and association of weighting factors to each of the components. In the following, we present some relevant examples extracted from literature, with an aim to identify key algorithms and data constraints of particular relevance to the successive work of DV 5.2.4.

Jedlovec et al. (2017) utilized a combination of satellite-derived ambient temperature maps, temperature thresholds derived from climatological percentiles of the ambient temperature and demographic information on population density, age and income for calculating heat wave risk maps (Figure 3).

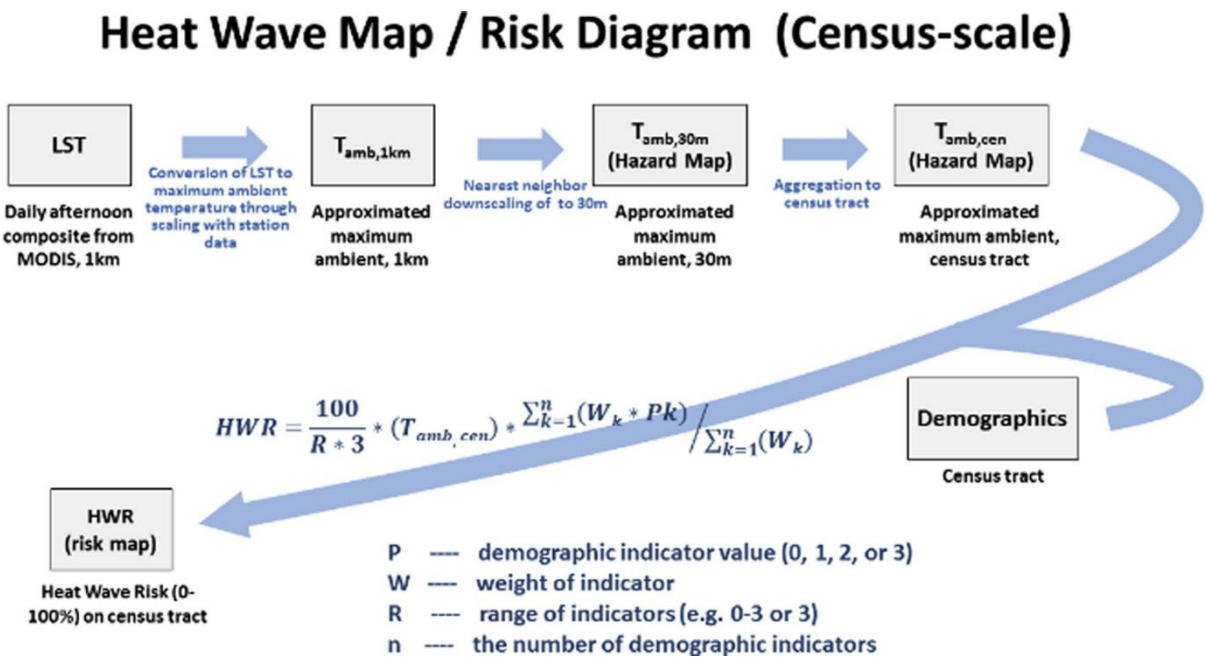

***Figure 3**. Schematic showing the combination of satellite data and demographic information to produce the Heat Wave Risk (HWR) product (Source: Jedlovec et al., 2017)*

Savić et al (2018) utilized a risk evaluation based on qualitative and quantitative procedures presented in the following Figure (Figure 4).

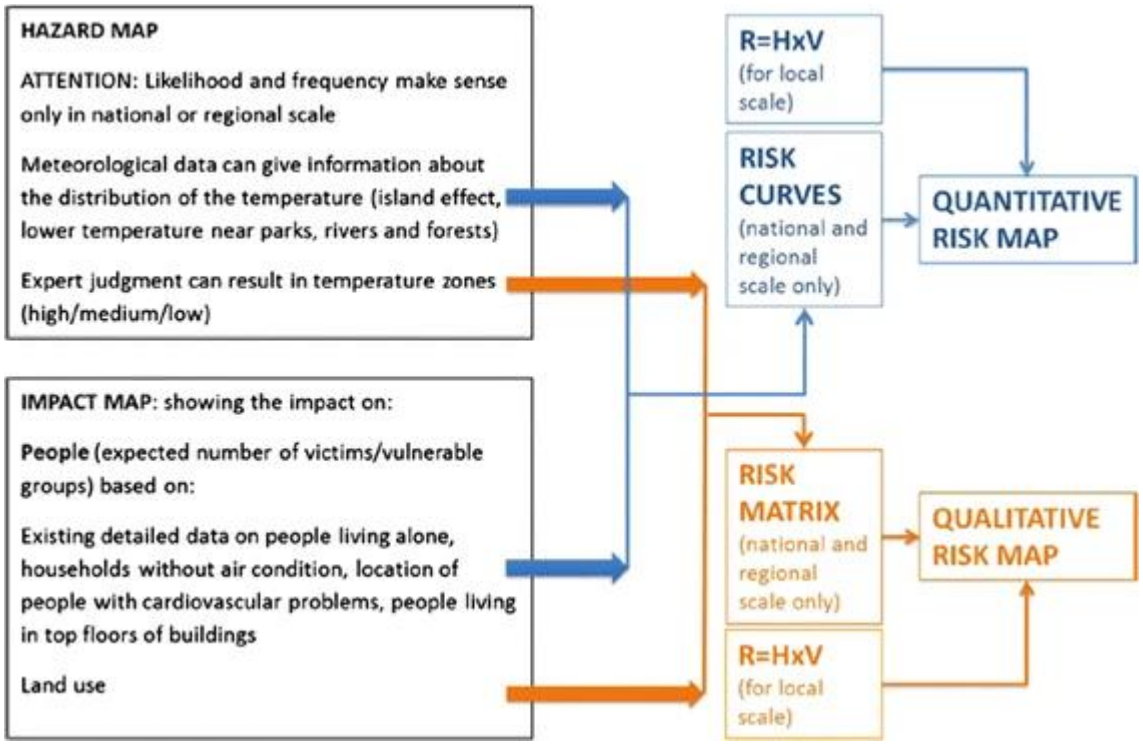

Figure 4. *Risk assessment and mapping procedure for heat waves utilized in Savić et al (2018).*

Their methodology combined description of land use based on the Local Climate Zone (Local Climate Zone) classification system (Stewart and Oke, 2012), air temperature data and specific criteria on duration and severity for identification of the days within very strong and intensive heat wave periods, and population data on mortality and spatial residence. On the basis of daily mortality data and urban heat island (UHI) intensity, the authors developed a risk matrix for the city of Novi Sad in Serbia, with the vertical axis showing the impact level in terms of average daily number of deaths in heatwave, and a standardized UHI intensity index value on the horizontal axis. Both axes were scaled from insignificant to very high, and the resulting risk level has five levels.

Tong et al. (2014) identified heatwaves as two or more days with mean temperature above the 98th percentile. After identification of the heat wave days, they were associated with a 1 (and non heatwave days were associated with 0). After that, heatwave effects on mortality and emergency hospital admissions were analysed with the Poisson General Additive Model. The sample population was categorized into different classes according to age. The results demonstrate that mortality and emergency hospital admissions significantly increase for heatwave days, with a higher vulnerability for the elderly group (≥75 years).

Buscail et al. (2012) utilized the risk framework developed by Crichton (1999), and represented the hazard as the increase in temperature as estimated from satellite derived land surface temperature, exposure from population census data from the areas affected by the hazard, and vulnerability from a combination of individual risk factors and building characteristics. The final risk map derives from the hazard index with the indices for exposure and vulnerability, following appropriate scaling through linear transformation. Four vulnerability dimensions (socio-economic status, extreme age –both extremes-, population density and building obsolescence) were combined. Specifically, socio-economic status was described through deprivation (Townsend score previously described), social

isolation (proportion of single households) and low education (proportion of population with no high school diploma). As scarcely inhabited areas would yield unreliable estimates for exposure and vulnerability, vulnerability and exposure indices were set to zero for areas with less than 200 inhabitants (Figure 5).

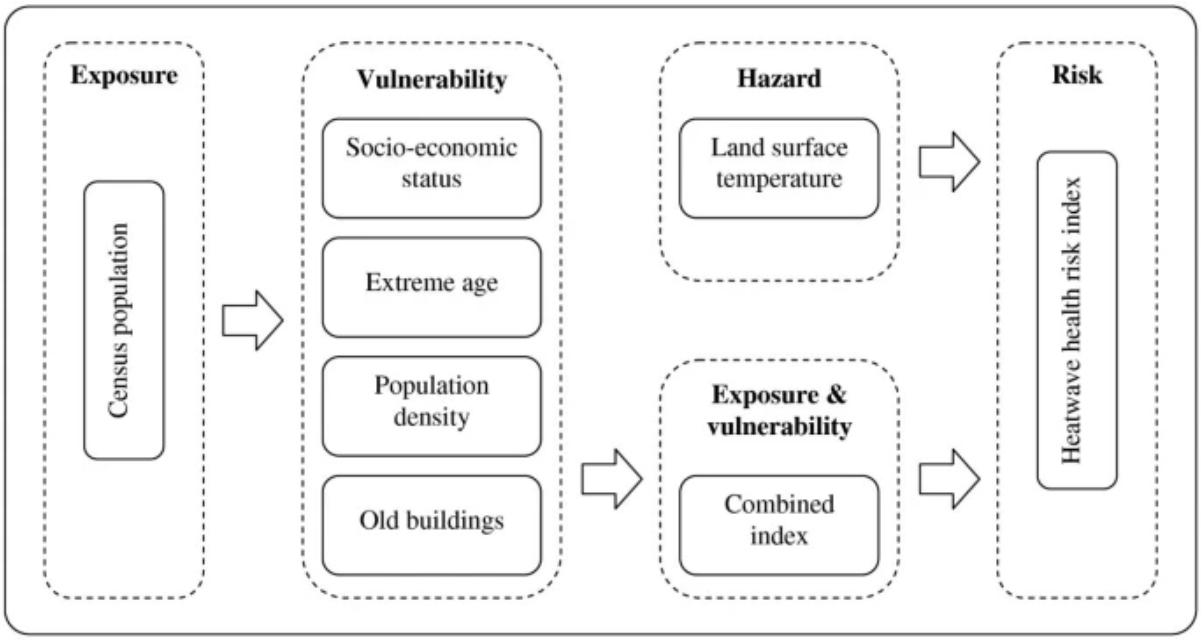

Figure 5. *Flowchart of the spatial risk assessment framework (Buscail et al. 2012).*

The heatwave risk model from Liu et al (2023) developed a heatwave risk index (HRI) combining heat wave days and population age as follows:

$HRI = days * (n_1 + n_2 + n_3)$

where n_1 is the total number of people of a street, n_2 is the number of young people aged 0–14 of a street, and n_3 is the elderly population aged above 65 of a street. days refers to the number of days with daily maximum temperature higher than 35 °C each year.

The risk framework of Holec et al. (2021) is particularly interesting as it obtains an adjusted hazard layer combining the hazard layer represented by surface temperature data with the mitigation layer describing tree density; exposure layer was represented by mobile phone density while vulnerability layer was represented by population over 65 years (Figure 6).

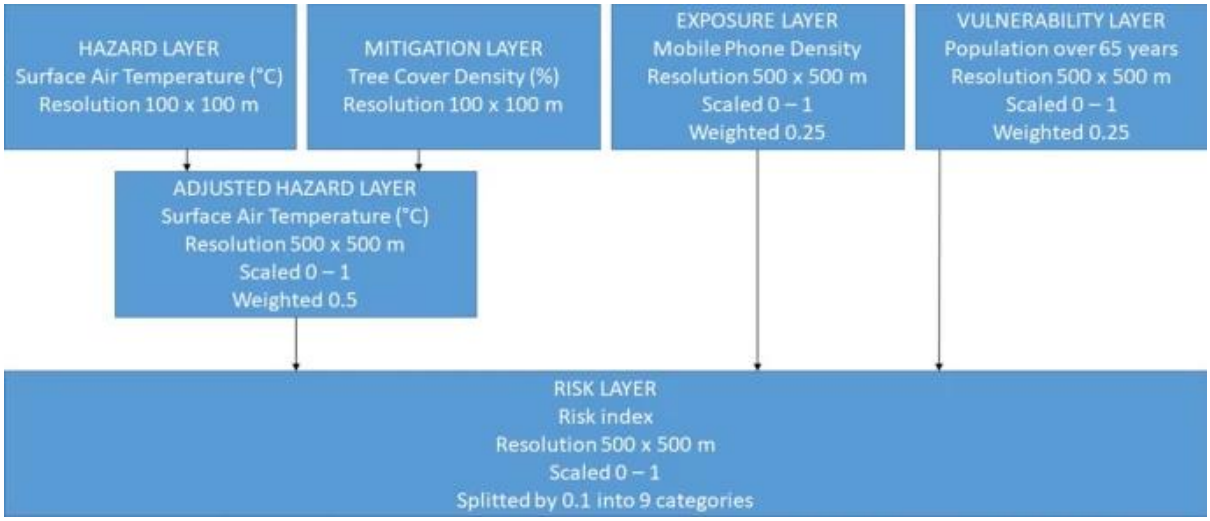

Figure 6. *Flow chart of risk index creation in Holec et al. (2021).*

Specifically, the calculation for the risk index followed the approach of Tomlinson et al. (2011) and Morabito et al. (2015). The modified hazard layer is represented by the UHI layer corrected with a tree vegetation layer (with a proper parameterization of the cooling effect associated with the tree cover), weighted with a 0.5 factor; the exposure layer, represented by base transceiver station centroids, weighted with a 0.25 factor; the vulnerability layer was described as the number of elderly people aged over 65, was weighted with 0.25 factor. Each layer was normalized with the min-max approach before weighting, and the risk index was calculated as the sum of weighted layers.

Aubrecht and Özceylan (2013) defined risk only from hazard and vulnerability. Heat wave indicators were chosen based on data availability and required spatial resolution. Specifically, a univariate temperature-based heat wave index was adopted, focused on thresholds on duration (at least 3 days) and intensity (daily maximum temperature above 30°C). Temperature maps were constructed by universal kriging applied to data coming from station observations in the study area. The Heat Stress Index was obtained by merging heat stress duration and frequency over time, normalized by maximum and minimum records ([value] − [min] / [max] − [min]), in order to have an index domain ranging from 0 to 1. Vulnerability was assessed through 6 indicators, namely age, social isolation, poverty, linguistic isolation, education and land cover characteristics. A composite heat stress vulnerability index was then obtained as the sum of the six indicators and normalized within the 0-1 range. The final heat stress risk index was calculated as the product of the two normalized risk components.

Dong et al. (2020) calculated an integrated score of heatwave-induced human health risk as follows:

$$HHR = \sqrt[3]{S \cdot E \cdot V}$$

Where HHR is the integrated risk score and S, E, V are the standardized indices for heat stress, exposure, vulnerability. Heat stress was expressed as the UTCI which combines a multi-node thermoregulation model with an adaptive clothing model (Bröde et al. 2012). Exposure was expressed through population density normalized with the min-max method. Social vulnerability was assessed through GDP per capita, convenience (distance) to reach medical assistance, age (proportion of people under 14 and over 65), proportion of female, proportion of population with education level below high school, proportion of population engaged in agriculture, forestry, animal husbandry and fishery. Following normalization, the indicators were subjected to PCA to extract a single social vulnerability score.

Alternative methods also exist, similarly combining hazard, exposure and vulnerability to heat waves into a unique index (e.g., Johnson et al., 2013; Keramitsoglu et al., 2013; Apreda et al., 2019; Zhang et al., 2019; Zemtsov et al., 2020; Wu et al., 2022; Cheval et al., 2023; Sabrin et al., 2022; Dai et al., 2021).

Table 16 shows a synthesis of the indicators and methods for heatwave risk calculation used in the previously mentioned papers.

Table 16. *Synthesis of indicators and methods for heatwave risk calculation used in the referenced papers.*

Hazard indicator	Exposure indicator	Vulnerability indicator	Risk algorithm	Reference
Land surface temperature	Census population	Deprivation (Townsend score); social isolation; education; age	Weighted combination of four vulnerability dimensions into unique exposed and vulnerability index; weighted hazard index.	Buscail et al., 2012
Satellite land surface temperature scaled with station data	Population density	percentage of the population over 65 years of age; mean income	Product of demographic and hazard indicators following scaling and weighting.	Jedlovec et al., 2017
Temperature mapping + satellite data on vegetation, imperviousness, elevation	Census population	Age; population density	Combination (product) of heatwave days and population age	Liu et al., 2023
Average Heatwave frequency, duration and intensity	Average of night time lights, People under 14 and People over 65	Average of Distance from water, Distance from hospital, Inverse(NDVI), and Inverse(GDP)	Average of indicators	Yin et al., 2020
air temperature differences between urban and non-urbanized areas	//	Land use, population, socio-economic status, building height and health status	Product of normalized indicators	Savić et al., 2018; Papathoma-Koehle et al., 2016a,b
//	Satellite land surface data; Proportional vegetation; Normalized difference	Population density, People living in poverty Unemployment rate	PCA on social and health vulnerability; regression analysis on environmental	Sabrin et al., 2022

	Water Index; Digital Elevation Model; Imperviousness	Minority races Foreign-born residents Vulnerable age (over 65, under 5) Health Uninsured Disability in adults Mode of commuting Structures built before 1980 % Population with Asthma % Population with Diabetes % Population with Heart diseases % Population with Obesity % Population with Chronic Obstructive Pulmonary Disease (COPD)	data for producing exposure index; risk as product of exposure and social and health vulnerability	
Intensity indicator from satellite land surface temperature	Population density	Population age; economic status; vegetation and water coverage;	Normalization of the indicators and weighted sum	Dai et al., 2021
cumulated number of cases when the satellite land surface temperature LST values exceed either 40 °C during the daytime , and/or 20 °C during nighttime		Average between land climate zone and population density	Product of hazard and vulnerability	Cheval et al., 2022
Physiologically equivalent temperature	Population density	Age; sedentary population; migrants; population income	Product of normalized indices	Zemtsov et al., 2020
Satellite daytime and nighttime	Population age; population income	Vegetation; water bodies; terrain	Product of normalized indices	Zhang et al., 2019

temperature; high temperature days (>35°C); air quality		conditions; housing condition; traffic convenience; medical facilities		
Very Hot Weather Warnings from the Hong Kong Observatory	Constituency population	Population age; education; employment status; income; percent of households	Compound hazard indicator and classification of hazard indicator into 5 classes	Johnson et al., 2016
Maximum apparent temperature and high nighttime temperatures; classification of severity with fuzzy logic model		population density and percentage of non-proper dwellings; fuzzy model	Sum of event scores provide the the monthly spatial distribution of heat wave hazard then multiplied with spatial distribution of population vulnerability	Keramitsoglou et al., 2013
Land surface temperature; parameterized cooling effect from trees	Building's volume and distance from ase Transceiver Station centroid	Population age	Product of scaled and normalized indicators	Holec et al., 2021
Universal Thermal Climate Index (UTCI)	Population density	Social vulnerability: Proportion of population under 14-year old (SV1) Proportion of population over 65-year old (SV2) Proportion of female population (SV3) Proportion of population with education level below high school (SV4) Proportion of population engaged in agriculture, forestry, animal	Cubic root of standardized indices	Dong et al., 2020

		husbandry and fishery (SV5) Adaptivity: GDP per capita (SV6)		

Quite similar approaches and necessity to associate weights and normalization to the indicators for developing risk indices are also shared by the risk of floods depicted in the other branch of the storyline (e.g., Vojtek, 2023; Usman Koje et al., 2021).

In spite of the differences described in terms of the indicators adopted and risk calculation algorithms, a few items emerge which have to be carefully taken into account in the choice of the risk calculation factor and based on the available data:

- Spatial resolution of the data is crucial: as the risk is a combination (sum or product) of the hazard, exposure and vulnerability, it is of paramount importance to search for the highest spatial resolution and disaggregation level for the input data.
- Spatial interpolation of point data sources (e.g., from station data) can be helpful especially for the hazard layer.
- The appropriate choice of the indicators adopted can partially mitigate the case of missing data. For example, if the application of a certain index requires data for solar radiation which are not available in the study area, the choice of an alternative indicator which is based on other meteorological variables can mitigate the lack of data.
- Data scarcity can be also mitigated through appropriate regionalization or downscaling (dynamic and/or statistical) techniques.
- The representation of the population vulnerability requires spatially resoluted (e.g., neighborhood) information on diverse categories such as age, education level, economic status.
- Parallel to the risk assessment, it is crucial to carry out an estimation of the uncertainty to be associated with hazard, exposure and vulnerability components.
- Risk can be assessed using quantitative, semi-quantitative and qualitative approaches, which correspond to different associated uncertainties.

9. Conclusions

By adopting a pragmatic approach based on risk storylines and related impact chains, this Deliverable showcases the development of a methodology for risk calculation suitable for the needs of RETURN and in particular within urban and metropolitan settlements. In practice, after selecting a relevant subset of risk storylines among those originally proposed in DV 5.2.1, indicators for each risk components are successively described, along with variables needed for their calculation. After that, algorithms and methods for risk assessment and quantification are presented utilizing the heatwave risk as a relevant example. After detailing the steps and methods for heatwave risk calculation, key principles and needs for the data sources, with specific references to uncertainty and constraints on data are drawn. In spite the Deliverable is far from complete as only two impact chains are herein described and the description of some specific items in the selected impact chains is still missing, the Deliverable successfully demonstrates the capabilities of the proposed approach for the development and the adoption of a standardized, flexible and modular methodology based on risk storylines and impact chains for the integration of heterogenous data in RETURN and for the development of smart data models for risk quantification, which will be the subject of following RETURN Deliverables (DV 5.2.4). This will be crucial for the development of the data platform in WP5, and for the development of risk models in WP3.

References

Aghamohammadi, N., Ramakreshnan, L., Fong, C.S., Noor, R.M., Hanif, N.R., Sulaiman, N.M., 2022. Perceived impacts of Urban Heat Island phenomenon in a tropical metropolitan city: perspectives from stakeholder dialogue sessions. Science of the Total Environment, 806, doi:10.1016/j.scitotenv.2021.150331

ANSI, ASHRAE, and M. Ashrae, 2017. "Standard 55—thermal environmental conditions for human occupancy." Amer. Soc. Heat, Refrigerat. Air Condition. Eng 1451992.

Apreda, C., D'Ambrosio, V., Di Martino, F., 2019. A climate vulnerability and impact assessment model for complex urban systems. Environmental Science & Policy, 93, 11-26, https://doi.org/10.1016/j.envsci.2018.12.016

Arbuthnott K, Hajat S., 2017. The health effects of hotter summers and heat waves in the population of the United Kingdom: a review of the evidence. Environ Health; 16:119, doi: 10.1186/s12940-017-0322-5.

Arribas, A., Fairgrieve, R., Dhu, T. et al., 2022. Climate risk assessment needs urgent improvement. Nat Commun 13, 4326 https://doi.org/10.1038/s41467-022-31979-w

Asim, K.M, Idris, A., Iqbal, T., Alvarez-Martinez, F., 2018. Seismic indicators based earthquake predictor system using Genetic Programming and AdaBoost classification. Soil Dynamics and Earthquake Engineering, 111, 1-7, https://doi.org/10.1016/j.soildyn.2018.04.020

Åström, D.O., Schifano, P., Asta, F., Lallo, A., Michelozzi, P., Rocklöv, J., Forsberg, B., 2015. The effect of heat waves on mortality in susceptible groups: a cohort study of a mediterranean and a northern European City. Environmental Health, 29:14:30., doi: 10.1186/s12940-015-0012-0.

Aubrecht, C, Özceylan, D., 2013. Identification of heat risk patterns in the U.S. National Capital Region by integrating heat stress and related vulnerability. Environment International, 56, 65-77, https://doi.org/10.1016/j.envint.2013.03.005

Basarin B, Lukić T, Matzarakis A., 2020. Review of Biometeorology of Heatwaves and Warm Extremes in Europe. Atmosphere, 11(12):1276. https://doi.org/10.3390/atmos11121276

Beevers, Popescu, I., Pregnolato, M., Liu, Y., Wright, N., 2022. Identifying hotspots of hydro-hazards under global change: A worldwide review. Front. Water, Sec. Water and Climate,Volume 4 - 2022 | https://doi.org/10.3389/frwa.2022.879536

Besagni, G., Borgarello, M., 2019. Measuring Fuel Poverty in Italy: A Comparison between Different Indicators. Sustainability, 11(10), 2732; https://doi.org/10.3390/su11102732

Bhatti, U.A., Marjan, S., Wahid, A., Syam, M., Huang, M., Tang, H., Hasnain, A., et al., 2023. The effects of socioeconomic factors on particulate matter concentration in China's: New evidence from spatial econometric model. Journal of Cleaner Production 417, 137969, https://doi.org/10.1016/j.jclepro.2023.137969

Boardman, B. Fuel poverty, 1991. From Cold Homes to Affordable Warmth; Pinter Pub. Limited: London, UK

Bouchama, A., Dehbi, M., Mohamed, G., Matthies, F., Shoukri, M., Menne, B., 2007. Prognostic factors in heat wave related deaths: a meta-analysis. Arch Intern Med 12, 167(20), 2170-6 doi: 10.1001/archinte.167.20.ira70009.

Brocherie, F., Millet, G.P., 2015. Is the Wet-Bulb Globe Temperature (WBGT) Index Relevant for Exercise in the Heat?. Sports Med 45, 1619–1621, https://doi.org/10.1007/s40279-015-0386-8

Bröde, P. et al. 2012. Deriving the operational procedure for the Universal Thermal Climate Index (UTCI). International Journal of Biometeorology, 56 (3), pp. 481-494, doi:10.1007/s00484-011-0454-1

Buscail, C., Upegui, E., Viel, J.-F., 2012. Mapping heatwave health risk at the community level for public health action. Int J Health Geogr 11, 38 https://doi.org/10.1186/1476-072X-11-38

Cai, W.J., et al., 2021. The 2020 China report of the Lancet Countdown on health and climate change. Lancet Public Health, 6 (1), pp. E64-E81. https://doi.org/10.1016/S2468-2667(20)30256-5

Caviedes-Voullième, D., Shepherd, T.G., 2023. Climate storylines as a way of bridging the gap between information and decision-making in hydrological risk. PLOS Climate, 2(8): e0000270 , https://doi.org/10.1371/journal.pclm.0000270

C40 Cities, 2018. CLIMATE CHANGE RISK ASSESSMENT GUIDANCE. Available online at https://cdn.locomotive.works/sites/5ab410c8a2f42204838f797e/content_entry5ab410fb74c4833febe6c81a/5b17dd2614ad660612c5dc54/files/C40_Cities_Climate_Change_Risk_Assessment_Guidance.pdf?1541689629, last accessed 16 October 2023

Cheval, S., et al., 2023. A country scale assessment of the heat hazard-risk in urban areas. Building and Environment, 229, 109892, https://doi.org/10.1016/j.buildenv.2022.109892

Costa IT, Wollmann CA, Writzl L, Iensse AC, da Silva AN, de Freitas Baumhardt O, Gobo JPA, Shooshtarian S, Matzarakis A., 2024. A Systematic Review on Human Thermal Comfort and Methodologies for Evaluating Urban Morphology in Outdoor Spaces. Climate, 12(3):30. https://doi.org/10.3390/cli12030030

Crepeau, P., Zhang, Z., Udyavar, R. et al., 2023. Socioeconomic disparity in the association between fine particulate matter exposure and papillary thyroid cancer. Environ Health 22, 20. https://doi.org/10.1186/s12940-023-00972-1

Crichton D, 1999. The risk triangle. Natural Disaster Management. Edited by: Ingleton J., London: Tudor Rose, 102-103.

Cutter, S.L., Boruff, B.J., and Shirley, W.L. 2003. Social vulnerability to environmental hazards. Social Science Quarterly 84(2): 242–261, https://doi.org/10.1111/1540-6237.8402002

Dai X, Liu Q, Huang C, Li H., 2021. Spatiotemporal Variation Analysis of the Fine-Scale Heat Wave Risk along the Jakarta-Bandung High-Speed Railway in Indonesia. International Journal of Environmental Research and Public Health; 18(22):12153. https://doi.org/10.3390/ijerph182212153

De Brujin, K.M., Lips, N., Gersonius, B., Middelkoop, H., 2016. The storyline approach: a new way to analyse and improve flood event management. Nat Hazards 81, 99–121 (2016). https://doi.org/10.1007/s11069-015-2074-2

De Medeiros, F. J., de Oliveira, C.P., Avila-Diaz, A., 2022. Evaluation of extreme precipitation climate indices and their projected changes for Brazil: From CMIP3 to CMIP6. Weather and Climate Extremes, 38, 100511, https://doi.org/10.1016/j.wace.2022.100511

Del Gaudio, C., De Martino, G., Di Ludovico, M. et al., 2019. Empirical fragility curves for masonry buildings after the 2009 L'Aquila, Italy, earthquake. Bull Earthquake Eng 17, 6301–6330 https://doi.org/10.1007/s10518-019-00683-4

Del Gaudio C, Di Ludovico M, Polese M, Manfredi G, Prota A, Ricci P, Verderame GM, 2020. Seismic fragility for Italian RC buildings based on damage data of the last 50 years. Bull Earthq Eng 18(5):2023–2059. https://doi.org/10.1007/s10518-020-00890-4

Di Napoli, C., Barnard, C., Prudhomme, C., Cloke, H.L., & Pappenberger, F. 2020. ERA5-HEAT: A global gridded historical dataset of human thermal comfort indices from climate reanalysis. Geoscience Data Journal, 8, 10 – 2, https://doi.org/10.24381/cds.553b7518

Di Napoli, C., Pappenberger, F., & Cloke, H.L. 2019. Verification of Heat Stress Thresholds for a Health-Based Heat-Wave Definition. Journal of Applied Meteorology and Climatology, 58, 1177–1194, https://doi.org/10.1175/JAMC-D-18-0246.1

Di Pasquale G., Orsini G. and Rome W. 2005. New Developments in Seismic Risk in Italy. Bullettin of Eqrthquake Engineering. 3: 101-128. https://doi.org/10.1007/s10518-005-0202-1

Dolce M, Speranza E, Giordano F, Borzi B, Bocchi F, Conte C, Di Meo A, Faravelli M, Pascale V 2019. Observed damage database of past Italian earthquakes: the Da.D.O. WebGIS. Bollettino di Geofisica Teorica ed Applicata 60(2):141–164

Dolce, M., Prota, A., Borzi, B. et al. Seismic risk assessment of residential buildings in Italy. Bull Earthquake Eng 19, 2999–3032 (2021). https://doi.org/10.1007/s10518-020-01009-5

Dong, J., et al. 2020. Heatwave-induced human health risk assessment in megacities based on heat stress-social vulnerability-human exposure framework. Landscape and Urban Planning, 203, 103907, https://doi.org/10.1016/j.landurbplan.2020.103907

Eini M.R., Rahmati, A., Salmani, H., Brocca, L., Piniewski, M., 2022. Detecting characteristics of extreme precipitation events using regional and satellite-based precipitation gridded datasets over a region in Central Europe. Science of The Total Environment 852,158497, https://doi.org/10.1016/j.scitotenv.2022.158497

EMA, 2018. Guideline on the environmental risk assessment of medicinal products for human use. Available online at: https://www.ema.europa.eu/en/environmental-risk-assessment-medicinal-products-human-use-scientific-guideline last accessed 16 October 2023

Epstein Y., and Moran, D.S. 2006. Thermal comfort and the heat stress indices. Industrial health 44.3: 388-398, https://doi.org/10.2486/indhealth.44.388

Faiella, I.; Lavecchia, L.; Borgarello, M., 2017. Una Nuova Misura Della Povertà Energetica Delle Famiglie (A New Measure of Households' Energy Poverty). Questioni di Economica e Finanza (Occasional Papers), 404, 1–16.

FEMA, 2003. Multi-Hazard Loss Estimation Methodology: Earthquake Model, HAZUS-MH Technical Manual. Washington, DC: Federal Emergency Management Agency. Available online at fema.gov/sites/default/files/2020-10/fema_hazus_earthquake_technical_manual_4-2.pdf last accessed 28 May 2024

FEMA, 2015. Rapid Visual Screening of Buildings for Potential Seismic Hazards: Supporting Documentation. Washington, DC: Federal Emergency Management Agency. Available online at Rapid Visual Screening of Buildings for Potential Seismic Hazards: Supporting Documentation (fema.gov), last accessed 28 May 2024

Field CB, Barros VR, Dokken DJ, Mach KJ, Mastrandrea MD, Bilir TE, et al., 2014. IPCC: climate change 2014: impacts, adaptation, and vulnerability. Part A: global and sectoral aspects, Contribution of working group II to the fifth assessment report of the intergovernmental panel on climate change. Cambridge and New York: Cambridge University Press; p. 1132.

Forastiere, F., Stafoggia, M., Tasco, C., Picciotto, S., Agabiti, N., Cesaroni, G., Perucci, C.A., 2017. Socioeconomic status, particulate air pollution, and daily mortality: differential exposure or differential susceptibility. Am J Ind Med.,50(3):208-16. doi: 10.1002/ajim.20368.

Fountain, M. Huizenga, C.e, 1997. "A thermal sensation prediction software tool for use by the profession". ASHRAE Transactions. 103 (2)

Frich, P., Alexander, L.V., Della-Marta, P.M., Gleason, B.E., Haylock, M.R., Tank, A.K., & Peterson, T.C., 2002. Observed coherent changes in climatic extremes during the second half of the twentieth century. Climate Research, 19, 193-212.

Frigerio, I., and M. De Amicis. 2016. Mapping social vulnerability to natural hazards in Italy: A suitable tool for risk mitigation strategies. Environmental Science & Policy 63: 187–196, https://doi.org/10.1016/j.envsci.2016.06.001

Frigerio, I., D. Strigaro, M. Mattavelli, S. Mugnano, and M. De Amicis. 2016. Construction of a social vulnerability index in relation to natural hazardousness for the Italian territory. Rendiconti Online Societa Geologica Italiana 39: 68–71,

Frigerio, I., Carnelli, F., Cabinio, M. et al., 2018. Spatiotemporal Pattern of Social Vulnerability in Italy. Int J Disaster Risk Sci 9, 249–262, https://doi.org/10.1007/s13753-018-0168-7

Gagge, A.P., Fobelets, A.P., & Berglund, L. 1986. A standard predictive index of human response to the thermal environment. Ashrae Transactions, 92, 709-731.

Gamble JL, Balbus J, Berger M, Bouye K, Campbell V, Chief K, et al. 2016. Populations of concern. The impacts of climate change on human health in the United States: a scientific assessment. Washington, DC: U.S. Global Change Research Program, p. 247–86. Available online at https://health2016.globalchange.gov/#:~:text=While%20all%20Americans%20are%20at,adults%2C%20vulnerable%20occupational%20groups%2C%20persons last accessed 19 October 2023

Garcia-Leon, D., Casanueva, A., Standardi, G., Burgstall, A., Flouris, A.D., Nybo, L., 2021. Current and projected regional economic impacts of heatwaves in Europe. Nature Communications, 12, 5807, https://doi.org/10.1038/s41467-021-26050-z

Garín, A., & Bejarán, R. 2003. Mortality rate and relative strain index in Buenos Aires city. International Journal of Biometeorology, 48, 31-36, https://doi.org/10.1007/s00484-003-0175-1

Giles, B.D., Balafoutis, C., & Maheras, P. 1990. Too hot for comfort: The heatwaves in Greece in 1987 and 1988. International Journal of Biometeorology, 34, 98-104, https://doi.org/10.1007/BF01093455

Grünthal, G., 1998. European Macroseismic Scale 1998 EMS-98. Available online at: title_ems98_msk (franceseisme.fr) last accessed 2 May 2024

Hajat A, Hsia C, O'Neill MS., 2015. Socioeconomic disparities and air pollution exposure: a global review. Curr Environ Health Rep., 2(4):440–50, doi: 10.1007/s40572-015-0069-5.

Hansen A, Bi P, Nitschke M, Pisaniello D, Newbury J, Kitson A., 2011. Older persons and heat-susceptibility: the role of health promotion in a changing climate. Health Promot J Aust. 2011;22(4):17–20, doi: 10.1071/he11417

Heindl, P., 2015. Measuring fuel poverty: General considerations and application to German household data. FinanzArchiv Public Financ. Anal., 71, 178–215

Henderson, S.B., McLeen, K.E., Lee, M.J., Kosatsky, T., 2022. Analysis of community deaths during the catastrophic 2021 heat dome. Early evidence to inform the public health response during

subsequent events in greater Vancouver, Canada. Environmental Epidemiology, 6(1), e189, DOI: 10.1097/EE9.0000000000000189

Hills, J., 2011. Fuel Poverty: The Problem and Its Measurement—Interim Report of the Fuel Poverty Review; CASE Report; Deparment for Energy and Climate Change: London, UK.

Holec, J., Šveda, M., Szatmári, D. et al., 2021. Heat risk assessment based on mobile phone data: case study of Bratislava, Slovakia. Nat Hazards 108, 3099–3120 https://doi.org/10.1007/s11069-021-04816-4

Höppe P., 1999. The physiological equivalent temperature - a universal index for the biometeorological assessment of the thermal environment. Int J Biometeorol.;43(2):71-5. doi: 10.1007/s004840050118. PMID: 10552310.

IPCC, 2019. Annex I: Glossary [van Diemen, R. (ed.)]. In: Climate Change and Land: an IPCC special report on climate change, desertification, land degradation, sustainable land management, food security, and greenhouse gas fluxes in terrestrial ecosystems [P.R. Shukla, J. Skea, E. Calvo Buendia, V. Masson-Delmotte, H.-O. Pörtner, D. C. Roberts, P. Zhai, R. Slade, S. Connors, R. van Diemen, M. Ferrat, E. Haughey, S. Luz, S. Neogi, M. Pathak, J. Petzold, J. Portugal Pereira, P. Vyas, E. Huntley, K. Kissick, M. Belkacemi, J. Malley, (eds.)]. Available online at https://www.ipcc.ch/site/assets/uploads/2019/11/11_Annex-I-Glossary.pdf last accessed 18 October 2023

IPCC, 2022. Annex II: Glossary [Möller, V., R. van Diemen, J.B.R. Matthews, C. Méndez, S. Semenov, J.S. Fuglestvedt, A. Reisinger (eds.)]. In: Climate Change 2022: Impacts, Adaptation and Vulnerability. Contribution of Working Group II to the Sixth Assessment Report of the Intergovernmental Panel on Climate Change [H.-O. Pörtner, D.C. Roberts, M. Tignor, E.S. Poloczanska, K. Mintenbeck, A. Alegría, M. Craig, S. Langsdorf, S. Löschke, V. Möller, A. Okem, B. Rama (eds.)]. Cambridge University Press, Cambridge, UK and New York, NY, USA, pp. 2897–2930, doi:10.1017/9781009325844.029.

ISTAT, 2011. 15° CENSIMENTO DELLA POPOLAZIONE E DELLE ABITAZIONI 2011. Available online at https://www.istat.it/it/censimenti-permanenti/censimenti-precedenti/popolazione-e-abitazioni/popolazione-2011, last accessed 28 May 2024

ISTAT, 2017. Household Budget Survey: Microdata for Research Purposes (Reference Year: 2015); ISTAT: Rome, Italy.

Jedlovec, G., Krane, D., Quattrocchi, D., 2017. Urban heat wave hazard and risk assessment. Results in Physics, 7, 4294-4295, https://doi.org/10.1016/j.rinp.2017.10.056

Ji, W., Zhu, Y., Du, H., Cao, B., Lian, Z., Geng, Y., Liu, S., Xiong, J., & Yang, C. 2022. Interpretation of standard effective temperature (SET) and explorations on its modification and development. Building and Environment, 210, 108714, https://doi.org/10.1016/j.buildenv.2021.108714

Johnson, K., Depietri, Y., and Breil, M., 2016. Multi-hazard risk assessment of two Hong Kong districts. International Journal of Disaster Risk Reduction, 19, 311-323, https://doi.org/10.1016/j.ijdrr.2016.08.023

Jones, R., and Boer, R. 2004. Assessing Current Climate Risks. Available online at https://www4.unfccc.int/sites/NAPC/Country%20Documents/General/apf%20technical%20paper04.pdf, last accessed 16 October 2023

Keramitsoglou, I., Kiranoudis, C.T., Maiheu, B. et al., 2013. Heat wave hazard classification and risk assessment using artificial intelligence fuzzy logic. Environ Monit Assess 185, 8239–8258. https://doi.org/10.1007/s10661-013-3170-y

Kim, K.-H., Kabir, E., Kabir, S., 2015. A review on the human health impact of airborne particulate matter. Environment International, 74, 136-143, http://dx.doi.org/10.1016/j.envint.2014.10.005

Krstic, N., Yuchi, W., Ho, H.C., Walker, B.B., Knudby, AJ., Henderson, S.B., 2017. The Heat Exposure Integrated Deprivation Index (HEIDI): A data-driven approach to quantifying neighborhood risk during extreme hot weather. Environment International, 109, 42-52. https://doi.org/10.1016/j.envint.2017.09.011

Lagomarsino, S., Giovinazzi, S., 2006. Macroseismic and mechanical models for the vulnerability and damage assessment of current buildings. Bull Earthquake Eng 4, 415–443. https://doi.org/10.1007/s10518-006-9024-z

Lavaysse, C., Cammalleri, C., Dosio, A., van der Schrier, G., Toreti, A., and Vogt, J., 2018. Towards a monitoring system of temperature extremes in Europe, Nat. Hazards Earth Syst. Sci., 18, 91–104, https://doi.org/10.5194/nhess-18-91-2018

Lee, D.H., 1965. Climatic stress indices for domestic animals. International Journal of Biometeorology, 9, 29-35.

Liu, M., Li, X., Chai, Z., Chen, A., Zhang, Y. and Zhang, Q. 2023. Dense Temperature Mapping and Heat Wave Risk Analysis Based on Multisource Remote Sensing Data, in IEEE Journal of Selected Topics in Applied Earth Observations and Remote Sensing, vol. 16, pp. 3148-3157, doi: 10.1109/JSTARS.2023.3260467.

López-Bueno, J.A., Navas-Martín, M.A., Linares, C., Mirón, J., Luna, M.Y., et al., 2021. Analysis of the impact of heat waves on daily mortality in urban and rural areas in Madrid. Environmental Research, 195, 110892, https://doi.org/10.1016/j.envres.2021.110892

Loridan, T., Coates, L., Frontiers, R., Argüeso, D., & Perkins-Kirkpatrick, S.E. 2016. The excess heat factor as a metric for heat-related fatalities: Defining heatwave risk categories. The Australian journal of emergency management, 31, 31-37.

Masterton, J. M. & Richardson, F. A., 1979. Humidex: a Method of Quantifying Human Discomfort Due to Excessive Heat and Humidity. Vol. 79 Environment Canada, Atmospheric Environment.

Matzarakis, A., Mayer, H., & Iziomon, M.G. 1999. Applications of a universal thermal index: physiological equivalent temperature. International Journal of Biometeorology, 43, 76-84, https://doi.org/10.1007/s004840050119

Mazziotta, M., and A. Pareto. 2015. On a generalized non-compensatory composite index for measuring socio-economic phenomena. Social Indicators Research 127(3): 983–1003.

McGregor, G.R., Bessmoulin, P., Ebi, K.L., & Menne, B. 2015. Heatwaves and health: guidance on warning-system development.

Mezősi , G., 2022. Meteorological hazards. In: Natural Hazards and the Mitigation of their Impact, pp. 97-136. Springer, Cham. https://doi.org/10.1007/978-3-031-07226-0_3

Middlemiss, L., 2017. A critical analysis of the new politics of fuel poverty in England. Crit. Soc. Policy, 37, 425–443.

Moore, R., 2012. Definitions of fuel poverty: Implications for policy. Energy Policy, 49, 19–26. https://doi.org/10.1016/j.enpol.2012.01.057

Mora, C., Dousset, B., Caldwell, I. et al., 2017. Global risk of deadly heat. Nature Clim Change 7, 501–506. https://doi.org/10.1038/nclimate3322

Nairn, J., & Fawcett, R.J., 2014. The Excess Heat Factor: A Metric for Heatwave Intensity and Its Use in Classifying Heatwave Severity. International Journal of Environmental Research and Public Health, 12, 227 – 253, https://doi.org/10.3390/ijerph120100227

Oliveira, A.R., Lopes, A., & Soares, A. 2022. Excess Heat Factor climatology, trends, and exposure across European Functional Urban Areas. Weather and Climate Extremes, 36, 100455, https://doi.org/10.1016/j.wace.2022.100455

O'Neill, M.S., Veves,A., Zanobetti, A., Sarnat, J.A., Gold, D.R., Economides, P.A., Horton, E.S., Horton, Schwartz, J., 2005. Diabetes Enhances Vulnerability to Particulate Air Pollution–Associated Impairment in Vascular Reactivity and Endothelial Function. Circulation 111, 2913-2920. https://doi.org/10.1161/CIRCULATIONAHA.104.517110

Osberghaus, D., and Abeling, T., 2023. Heat vulnerability and adaptation of low-income households in Germany. Global Environmental Change, 72, 102446. https://doi.org/10.1016/j.gloenvcha.2021.102446

Oven, K.J., Curtis, S.E., Reaney, S., Riva, M., Stewart, M.G., Ohlemüller, R., et al., 2012. Climate change and health and social care: Defining future hazard, vulnerability and risk for infrastructure systems supporting older people's health care in England. Applied Geography 33, 16-24, doi:10.1016/j.apgeog.2011.05.012

Papathoma-Köhle M, Promper C, Bojariu R, Cica R, Sik A, Perge K, László P, Balázs Czikora E, Dumitrescu A, Turcus C, Birsan MV, Velea L, Glade T, 2016a. A common methodology for risk assessment and mapping for south-east Europe: an application for heat wave risk in Romania. Nat Hazards 82:S89–S109. https://doi.org/10.1007/s11069-016-2291-3

Papathoma-Köhle M, Promper C, Glade T, 2016b. A common methodology for risk assessment and mapping of climate change related hazards-implications for climate change adaptation policies. Climate 4:8. https://doi.org/10.3390/cli4010008

Pasquale, G.D., Orsini, G. & Romeo, R.W.. 2005. New Developments in Seismic Risk Assessment in Italy. Bull Earthquake Eng 3, 101–128. https://doi.org/10.1007/s10518-005-0202-1

Paterson, S.K., Godsmark, C.N., 2020. Heat-health vulnerability in temperate climates: lessons and response options from Ireland. Global Health 16, 29, https://doi.org/10.1186/s12992-020-00554-7

Rademaekers, K.; Yearwood, J.; Ferreira, A.; Pye, S.; Ian Hamilton, P.; Agnolucci, D.G.; Karásek, J.; Anisimova, N. Selecting Indicators to Measure Energy Poverty Rotterdam; Framework Contract ENER/A4/516-2014; Trinomics: Rotterdam, The Netherlands, 2016.

Ratter-Rieck, J.M., Roden, M., Herder, C., 2023. Diabetes and climate change: current evidence and implications for people with diabetes, clinicians and policy stakeholders. Diabetologia 66(6), 1003-1015, doi: 10.1007/s00125-023-05901-y

Rey, G., et al., 2009. Heat exposure and socio-economic vulnerability as synergistic factors in heat-wave-related mortality. Eur J Epidemiol.24(9):495-502. doi: 10.1007/s10654-009-9374-3. Epub 2009 Jul 30.

Richardson K, Moore P, Peklar J, Galvin R, Bennett K, Kenny R. Polypharmacy in adults over 50 in Ireland: opportunities for cost saving and improved healthcare. In: The Irish longitudinal study on ageing, Lincoln Place, Trinity College Dublin, Dublin, 2; 2012.

Romero, J.C., Linares, P., López Otero, X., Labandeira, X., Pérez Alonso, A., 2015. Energy Poverty in Spain, Economic Analysis and Proposals for Action; Economics for Energy: Madrid, Spain.

Rosano et al., 2020. Aggiornamento e revisione dell'indice di deprivazione italiano 2011 a livello di sezione di censimento. Epidemiol Prev, 44 (2-3): 162-170

Robinson, P.J., 2021. On the definition of a heat wave. Journal of Applied Meteorology and Climatology, 40, 4, 762-775, https://doi.org/10.1175/1520-0450(2001)040<0762:OTDOAH>2.0.CO;2

Rosti, A., Rota, M. & Penna, A., 2022. An empirical seismic vulnerability model. Bull Earthquake Eng 20, 4147–4173. https://doi.org/10.1007/s10518-022-01374-3

Russo, S., A. Dosio, R. G. Graversen, J. Sillmann, H. Carrao, M. B. Dunbar, A. Singleton, P. Montagna, P. Barbola, and J. V. Vogt, 2014, Magnitude of extreme heat waves in present climate and their projection in a warming world, J. Geophys. Res. Atmos., 119, 12,500–12,512, doi:10.1002/2014JD022098.

Sabrin, S., Karimi, M., Nazari, R., 2022. Modeling heat island exposure and vulnerability utilizing earth observations and social drivers: A case study for Alabama, USA. Building and Environment 226, 109686, https://doi.org/10.1016/j.buildenv.2022.109686

Savić, S., Marković, V., Šećerov, I. et al., 2018. Heat wave risk assessment and mapping in urban areas: case study for a midsized Central European city, Novi Sad (Serbia). Nat Hazards 91, 891–911. https://doi.org/10.1007/s11069-017-3160-4

Schulte P, Bhattacharya A, Butler C, Chun H, Jacklitsch B, Jacobs T, et al., 2016. Advancing the framework for considering the effects of climate change on worker safety and health. J Occ Environ Hyg., 13(11):847–65, doi: 10.1080/15459624.2016.1179388

Shepherd, T., et al., 2018. Storylines: an alternative approach to representing uncertainty in physical aspects of climate change. Climatic Change 151, 555–571 (2018). https://doi.org/10.1007/s10584-018-2317-9

Spalt EW, Curl CL, Allen RW, Cohen M, Williams K, Hirsch JA, et al., 2016. Factors influencing time-location patterns and their impact on estimates of exposure: the multi-ethnic study of atherosclerosis and air pollution (MESA air). J Expo Sci Environ Epidemiol., 26(4):341–8., doi: 10.1038/jes.2015.26

Staiger, H., Laschewski, G. & Grätz, A., 2012. The perceived temperature – a versatile index for the assessment of the human thermal environment. Part A: scientific basics. Int J Biometeorol 56, 165–176, https://doi.org/10.1007/s00484-011-0409-6

Steadman, R.G. A Universal Scale Of Apparent Temperature. J. Clim. Appl. Meteorol. 1984, 23, 1674–1687.

Stewart ID, Oke TR, 2012. Local climate zones for urban temperature studies. Bull Am Meteorol Soc 93:1879–1900. https://doi.org/10.1175/BAMS-D-11-00019.1

Stucchi M. Camassi R. Rovida A. Locati M. Ercolani E. Meletti C. Migliavacca P. Bernardini F. Azzaro R. (2007). DBMI04, il database delle osservazioni macrosismiche dei terremoti italiani

utilizzate per la compilazione del catalogo parametrico CPTI04, Quad. Geofis. 49, 38, http://emidius.mi.ingv.it/DBMI04/.

Stucchi M., Meletti C., Montaldo V., Crowley H., Calvi G.M., Boschi E., 2011. Seismic Hazard Assessment (2003-2009) for the Italian Building Code. Bulletin of the Seismological Society of America 101, 4, 1885-1911. https://doi.org/10.1785/0120100130

Stull R 2011: Wet-bulb temperature from relative humitidy and air temperature. J Appl. Meteorology and climatoloy, 50, 2267-2269.

Tartarini, F., and Schiavon, S., 2020. "pythermalcomfort: A Python package for thermal comfort research." SoftwareX 12, 100578, https://doi.org/10.1016/j.softx.2020.100578

Tartarini, Federico, et al., 2020. "CBE Thermal Comfort Tool: Online tool for thermal comfort calculations and visualizations." SoftwareX 12, 100563, https://doi.org/10.1016/j.softx.2020.100563

Thom EC 1959. The discomfort index. Weatherwise 12.2: 57-61.

Tomlinson CJ, Chapman L, Thornes JE, Baker CJ, 2011. Including the urban heat island in spatial heat health risk assessment strategies: a case study for Birmingham. UK. Int J Health Geographics 10(1):1–14. https://doi.org/10.1186/1476-072X-10-42

Tong, S., Wang, X.Y., FitzGerald, G. et al., 2014. Development of health risk-based metrics for defining a heatwave: a time series study in Brisbane, Australia. BMC Public Health 14, 435. https://doi.org/10.1186/1471-2458-14-435

Townsend P, 1987. Deprivation. J Soc Policy, 16: 125-146. 10.1017/S0047279400020341.

Trajkovic, S., Kisi, O., Markus, M., Tabari, H., Gocic, M., Shamshirband, S., 2016. Hydrological Hazards in a Changing Environment: Early Warning, Forecasting, and Impact Assessment. Advances in Meteorology 2016, 2752091, https://doi.org/10.1155/2016/2752091

UNDRR-ISC, 2021. “Hazard Information Profiles - Supplement to UNDRR-ISC Hazard Definition & Classification Review.” UNDRR-ISC.

UNISDR, 2015. Sendai Framework for Disaster Risk Reduction 2015-2030. 32 pp Available online at https://www.undrr.org/publication/sendai-framework-disaster-risk-reduction-2015-2030 last accessed 18 October 2023

Usman Kaoje I, Abdul Rahman MZ, Idris NH, Razak KA, Wan Mohd Rani WNM, Tam TH, Mohd Salleh MR., 2021. Physical Flood Vulnerability Assessment using Geospatial Indicator-Based Approach and Participatory Analytical Hierarchy Process: A Case Study in Kota Bharu, Malaysia. Water., 13(13):1786. https://doi.org/10.3390/w13131786

Van der Hurk, B.J.J.M., et al., 2023. Climate impact storylines for assessing socio-economic responses to remote events. Climate Risk Management, 40, 100500, https://doi.org/10.1016/j.crm.2023.100500

Vojtek, M. Indicator-based approach for fluvial flood risk assessment at municipal level in Slovakia. Sci Rep 13, 5014 (2023). https://doi.org/10.1038/s41598-023-32239-7

Yin C, Yang F, Wang J, Ye Y., 2020. Spatiotemporal Distribution and Risk Assessment of Heat Waves Based on Apparent Temperature in the One Belt and One Road Region. Remote Sensing; 12(7):1174. https://doi.org/10.3390/rs12071174

Wang, L.-N., Chen, X.-H., Shao, Q.-X., Li, Y., 2015. Flood indicators and their clustering features in Wujiang River, South China. Ecological Engineering, 76, 66-74, https://doi.org/10.1016/j.ecoleng.2014.03.018

Watts, J.D., & Kalkstein, L.S. 2004. The Development of a Warm-Weather Relative Stress Index for Environmental Applications. Journal of Applied Meteorology, 43, 503-513. https://doi.org/10.1175/1520-0450(2004)043%3C0503:TDOAWR%3E2.0.CO;2

WHO, 2015. Outdoor Air Pollution. IARC Monographs on the Evaluation of Carcinogenic Risks to Humans Volume 109, ISBN 978-92-832-0147-2, available online at https://publications.iarc.fr/538 last accessed 19 October 2023

WHO, 2023a. https://www.who.int/health-topics/air-pollution#tab=tab_1, last accessed 17 October 2023

WHO, 2023b. https://www.who.int/india/heat-waves last accessed 18 October 2023

Witherspoon and Goldman, 1974. Indices for thermal stress. ASHRAE Bull. (No. LO-73-8) (1974), pp. 5-13

WMO, 1992. International Meteorological Vocabulary. WMO No. 182. Available online at: International meteorological vocabulary (WMO-No. 182) last accessed 30 April 2024

World Meteorological Organization, 2009. Guidelines on Analysis of extremes in a changing climate in support of informed decisions for adaptation. World Meteorological Organization.

WMO, 2012. Urban flood risk management. APFM Technical Document No. 11. Available online at: https://library.wmo.int/viewer/37067?medianame=ifmts_6_#page=3&viewer=picture&o=bookmark&n=0&q=, last accessed 16 May 2024

WMO, 2023. Guidelines on the definition and characterization of extreme weather and climate events. WMO No. 1310 report. Available online at: Guidelines on the Definition and Characterization of Extreme Weather and Climate Events (WMO-No. 1310) last accessed 30 April 2024

Woo, Gordon, and Neil F. Johnson. 2023. Stochastic Modeling of Possible Pasts to Illuminate Future Risk." In The Oxford Handbook of Complex Disaster Risks and Resilience, edited by James M. Shultz and Andreas Rechkemmer, 1st ed., C12P1-C12S11. Oxford University Press. https://doi.org/10.1093/oxfordhb/9780190466145.013.12

Wu X, Liu Q, Huang C, Li H., 2022. Mapping Heat-Health Vulnerability Based on Remote Sensing: A Case Study in Karachi. Remote Sensing.; 14(7):1590. https://doi.org/10.3390/rs14071590

Zare, S., Hasheminejad, N., Shirvan, H.E., Hemmatjo, R., Sarebanzadeh, K., & Ahmadi, S. 2018. Comparing Universal Thermal Climate Index (UTCI) with selected thermal indices/environmental parameters during 12 months of the year. Weather and climate extremes, 19, 49-57, https://doi.org/10.1016/j.wace.2018.01.004

Zauli Sajani, S. et al. 2016. UHI in the Metropolitan Cluster of Bologna-Modena: Mitigation and Adaptation Strategies. In: Musco, F. (eds) Counteracting Urban Heat Island Effects in a Global Climate Change Scenario. Springer, Cham. https://doi.org/10.1007/978-3-319-10425-6_6

Zemtsov, S., et al., 2020. Intraurban social risk and mortality patterns during extreme heat events: A case study of Moscow, 2010-2017. Health & Place, 66, 102429, https://doi.org/10.1016/j.healthplace.2020.102429

Zhang Y, Yu C, Wang L., 2017. Temperature exposure during pregnancy and birth outcomes: an updated systematic review of epidemiological evidence. Environ Pollut., 225:700–12, doi: 10.1016/j.envpol.2017.02.066.

Zhang W., Zheng Y., Chen F., 2019. Mapping heat-related health risks of elderly citizens in mountainous area: A case study of Chongqing, China. Science of the Total Environment 663, 852-866, https://doi.org/10.1016/j.scitotenv.2019.01.240

Zuccaro G., and F. Cacace 2011. Seismic casualty evaluation: the Italian model, an application to the L'Aquila 2009 event, In Human Casualties in Earthquakes: progress in modelling and mitigation, R. Spence, E. So, and C. Scawthorn (Editors), Springer, London, UK.